Flux of nutrients and mercury from an Arctic seabird colony to the coastal food web

Eirik Aasmo Finne

Master Thesis
Ecology and evolution
60 credits

IBV
CEES

UNIVERSITY OF OSLO

May 2019

Title: Flux of nutrients and mercury from an Arctic seabird colony to the coastal food web

Author: Eirik Aasmo Finne

Supervisors: Joël Durant (University of Oslo)

                  Amanda Poste (Norwegian institute for Water Research)

                  Øystein Varpe (University Centre in Svalbard)

II

Acknowledgements

Abstract

Seabirds bring substantial amounts of nitrogen (N) and phosphorous (P) from sea to their breeding colonies. On Svalbard, previous research has focused on the ornithogenic fluxes from sea to land, but little is known of the effects of seabird colonies on nearby marine environments. External nutrient input has potential to increase primary production during summer, when nutrient availability is the limiting factor. Seabirds can also function as biovectors for transport of contaminants, such as mercury (Hg), from their foraging areas to the colony, but there are uncertainties on how the presence of these colonies could affect contaminant accumulation in affected coastal food webs. The objective of this thesis is therefore twofold: (i) characterising the nutrient and Hg flux from a seabird colony, and (ii) investigating the response in a nearby coastal ecosystem.

To study these seabird driven fluxes, a mixed colony of Black-legged kittiwakes (*Rissa tridactyla*) and Brünnich's guillemots (*Uria lomvia*) at Alkhornet, west coast of Spitsbergen, was visited on five occasions from June to September 2018. Water was collected for chemical analysis from three streams influenced by the seabird colony and in three control streams, with little seabird presence. In the adjacent coastal ecosystem, stable carbon and nitrogen isotope analysis (δ^{15}N and δ^{13}C) was used to assess the ornithogenic nutrient uptake by primary producers (*Acrosiphonia* sp.) and its propagation to higher trophic levels (amphipods). Concentrations of methyl-mercury (MeHg) were also determined in a primary consumer (amphipods).

The seabird influenced streams had much higher (5-100 fold) concentrations of organic carbon and dissolved N and P than control streams. Aqueous Hg was positively related to organic matter in colony-influenced streams, while turbidity was a better predictor for aqueous Hg for control streams. An ornithogenic signal (higher δ^{15}N) was found in all biota collected from the seabird influenced sites. *Acrosiphonia* close to the colony had lower C:N ratios than specimens collected from control sites, indicating higher N-availability. Low MeHg concentrations were observed in amphipods close to the colony, possibly due to availability of high-quality food, which could lead to high trophic efficiency and therefore lower bioaccumulation of MeHg. In light of ongoing climate change and declining seabird populations, effort should also be put on understanding potential future changes in ornithogenic fluxes from land to sea, and the implications for adjacent coastal ecosystems.

Table of content

1 Introduction

Approximately 3 million pairs of seabirds breed on Svalbard, accounting for more than half the total number in Norway (Anker-Nilssen *et al.* 2015). Together with populations worldwide, many of the colonies in Norway have experienced drastic declines in recent years (Anker-Nilssen *et al.* 2018). Globally, a 70% decrease in the number of seabirds from 1950 to 2010 has been estimated (Paleczny *et al.* 2015). In Norway, this negative development has been most prevalent along the mainland coast, but the same trend is emerging among some populations on Svalbard (Anker-Nilssen *et al.* 2018). As seabirds are considered to be good indicators of the health of marine ecosystem (Parsons *et al.* 2008), a negative population trend is concerning not only for the persistence of the seabird populations, but also for the overall state of the ecosystem. Seabirds are important consumers in the marine food webs, consuming upwards of 1 million tonnes annually of fish and invertebrates in the Barents sea (Barrett *et al.* 2002). In addition to this top down effect, seabirds can also affect ecosystems through bottom up processes.

A common strategy for many seabird species is to congregate in large colonies to breed. By leaving droppings and remains in the vicinity of the colony, seabirds bring nutrients across the boundary between sea and land. Otero *et al.* (2018) estimates a global annual deposition of 591 Gg nitrogen and 99 Gg phosphorus in the world's breeding colonies. This is a considerable amount considering that this nitrogen transport is equivalent to 1% of the yearly terrestrial biological nitrogen fixation in the world (Vitousek *et al.* 2013). Furthermore, these ornithogenic nutrient fluxes are mainly concentrated poleward (Otero *et al.* 2018), where other sources of biological accessible nitrogen are generally scarce (Galloway *et al.* 2004).

Some generalisations can be made on the fate of nitrogen from the seabird droppings. Washing out during precipitation events and volatilisation of ammonia (NH_3) from uric acid and other nitrogen-compounds in the guano are important pathways for further nitrogen distribution to the vicinity of colonies. The speed of this processes is however dependent on temperature, pH, precipitation and substrate type. NH_3 typically has a short atmospheric lifetime and will be redeposited within a few hundred meters to a few km (Pitcairn *et al.* 2002). Ammonium (NH_4^+) from guano and deposited NH_3 can be further oxidized to nitrate (NO_3^-) and nitrite (NO_2^-). These are among the most important fertilizers for both terrestrial

and aquatic primary producers (*e.g.* Glibert *et al.* 2016). In the surroundings of Arctic bird cliffs, intensely green and lush vegetation thrive, making the effect of seabird fertilisation striking. With increasing distance from the colony, a gradient in seabird influence on terrestrial and limnic environments can be observed, manifested in altered species abundance, composition and physical characteristics, as well as stoichiometry of soil and water (Duda *et al.* 2018; González-Bergonzoni *et al.* 2017; Richter *et al.* 2017). In this way, seabirds can function as ecosystem engineers.

Seabird driven transport of energy and matter from sea to land is well documented on Svalbard. However, the nutrient runoff from Arctic seabird colonies to the nearby coastal environment, with its effects, are relatively understudied (Berchenko *et al.* 2017; Bouchard Marmen *et al.* 2017). External (allochthonous) inputs of nutrients in the summer months have the potential to increase the primary production, and ornithogenic nutrients have been proposed to be one such source (Shatova *et al.* 2017; Zmudczyńska-Skarbek *et al.* 2015). Indeed, previous work has suggested that the high numbers of seabirds breeding in Hornsund contribute to a higher annual production relative to another west-Spitsbergen fjord, Kongsfjorden (Smoła *et al.* 2017). The potential response in coastal ecosystems close to seabird colonies can be expected to vary greatly from site to site on Svalbard. Different species and population numbers will affect the composition and amount of ornithogenic matter (Zwolicki *et al.* 2016). Topography, soil structure and hydrological regime, combined with the distance between colony and coast, will further determine the terrestrial retention and release to the coast.

Furthermore, a seasonal perspective is important in understanding both the nature of these ornithogenic fluxes and the potential response of marine ecosystems. Among the most numerous seabirds on Svalbard are Black-legged kittiwake (*Rissa tridactyla*) and Brünnich's guillemot (*Uria lomvia*). Both species arrive at their colonies in Svalbard by April, before egg laying starts early June (Witherby 1963). The chicks then hatch in the first or second week of July (Burr *et al.* 2016). While the guillemot chicks leave their nests after roughly 20 days and before they are fully fledged, the kittiwake nestlings will stay until they are fledged at five or six weeks of age (Witherby 1963). Bird phenology, with seasonal changes in activity and colony presence, infer a seasonality in the ornithogenic nutrient input to the vicinity. Other factors, such as the onset of the melting period, are then highly important for the further propagation of these fluxes to the sea.

To isolate the effect of the colony on nutrient fluxes to coastal waters, other sources of nutrients to the runoff need to be considered. Atmospheric NO_X deposition is associated with precipitation events, leading to higher concentrations in meltwater from snowpacks than in glacier meltwater (Tranter *et al.* 2002). Furthermore, nitrogen fixation by cyanobacteria and other diazotrophs has been shown to be an important source of bioavailable nitrogen in Arctic tundra soil (Rousk *et al.* 2017). Soil and bedrock can have high phosphorous content, which can be released to streams by weathering processes. However, while phosphate (PO_4^{3-}) is readily available for uptake in primary producers, many geochemical forms of phosphorous (e.g. bound to calcium, iron or aluminium) are scarcely available (Reynolds & Davies 2001). Chemical weathering of rocks is also a major source of silicate in rivers, essential for silicifying phytoplankton. The silicate concentrations can increase with greater water flow, as increased erosion expose a larger mineral surface area and silicate dissolution rate increases (Anderson 2005).

The response of coastal ecosystems to external nutrient input is further determined by the timing of the fluxes. Seasonality is a key driver in Arctic marine ecosystems, where the extreme change in light condition is of high importance for primary production rates and life histories. Excess nutrients accumulated during winter, coupled with a rapid increase in irradiance during spring leads to a large increase in production. As the summer proceeds, primary production typically becomes limited by nutrient availability, particularly nitrogen, silicate and to some extent phosphorous. Since the highest intensity of the ornithogenic nutrient fluxes can be expected to coincide with the onset of the marine nutrient depleted state, it strengthens the potential of seabirds to increase production in coastal ecosystems.

In addition to nutrients, seabirds can be biovectors for contaminant transport from sea to land. As seabirds are typically at high trophic levels in marine food webs they are susceptible to bioaccumulative compounds. Elevated contaminant levels have previously been documented in terrestrial and aquatic artic environments close to bird cliffs on Svalbard (Kristiansen 2017) and in other parts of the Arctic (Blais *et al.* 2005; Choy *et al.* 2010). One of these contaminants is mercury, of which methylated mercury (MeHg) is specially concerning due to its severe neurotoxicity, combined with bioaccumulation and biomagnification properties (Lehnherr 2014). Since inputs of anthropogenic mercury from local sources in the Arctic is limited, most of the mercury originates as long distance transported Hg(0) (Durnford *et al.* 2010). After deposition of elemental mercury, iron- and

sulphate reducing bacteria can transform it to MeHg (Lehnherr 2014). The role of seabirds as a contaminant biovector must be seen in light of ornithogenic nutrient flux. Although we might anticipate higher contaminant input to seabird influenced area, higher nutrient inputs may sustain higher growth rates in seabird influenced areas, potentially leading to lower bioaccumulation due to growth dilution (Pickhardt *et al.* 2002).

1.1 Aim

With the present study, the aim is to quantify the flux of orntithogenic nutrients and mercury to the coastal ecosystems. Alkhornet, one of the largest bird colonies on the west coast of Spitsbergen, Svalbard, was chosen as a study site. The influence of seabirds on streams draining the area will be characterised and coastal biota will be analysed for their response to ornithogenic fluxes of nutrients and mercury.

To reach these aims, four hypotheses were formulated:

1. Runoff from seabird influenced streams will have high concentrations of bioavailable nutrients, organic carbon and mercury compared to unimpacted streams.
2. Nutrient concentrations, organic content and mercury concentrations in the seabird influenced streams will display seasonal variation. Nutrient concentrations will decrease after the seabirds leave the colony and will be negatively correlated with discharge due to dilution. Organic carbon and concentrations of total mercury will be positively correlated with discharge as this promotes erosion.
3. Utilisation of seabird derived nutrients can be traced in marine costal organisms close to the colony
4. Mercury accumulation will be higher in biota close to the colony.

2 Methods

2.1 Study site
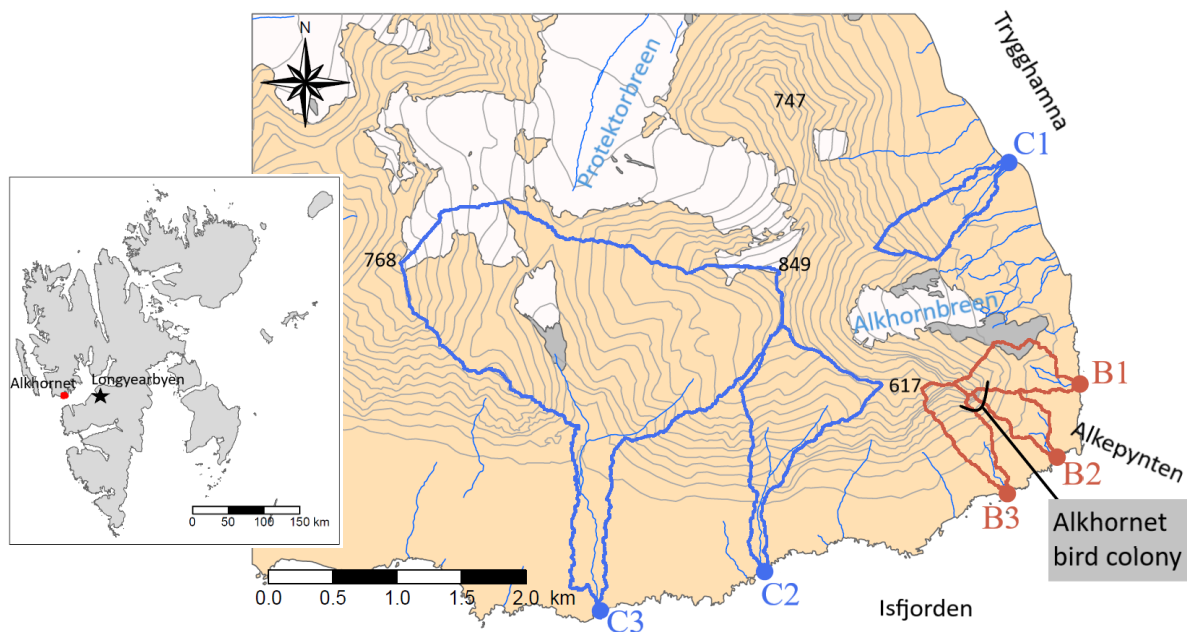
Figure 1: Study area with station numbers and corresponding catchment areas. C1, C2 and C3 (blue) are control stations, while B1, B2 and B3 (red) are the bird influenced stations. As shown on the overview map, the study site is located almost 50 km west of Longyearbyen, the largest town on Svalbard. © *Norwegian Polar Institute*.

The study site chosen for this project is Alkhornet, one of largest bird cliffs near Isfjorden, Svalbard (Figure 1). Located on the north side of the Isfjorden fjord mouth, Alkhornet displays a characteristic rock wall, peaking at 431 meters above sea level (Figure 2). Here, Brünnich's guillemot (*Uria lomvia*) and Black legged kittiwake (*Rissa tridactyla*) are the most numerous seabirds (Camphuysen & den Ouden 1995). While the wall is the area with highest seabird abundance, some pairs
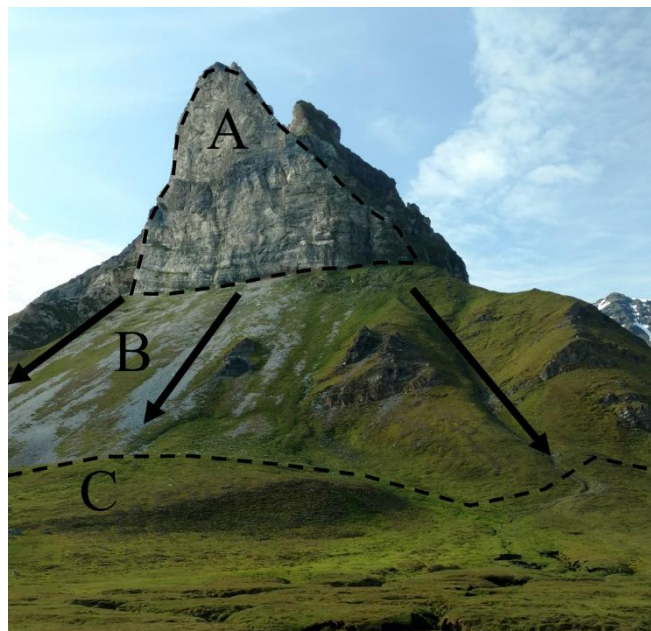
Figure 2: Alkhornet seen from the east, close to station B1. A: The main rock wall with the colony. Several bird pairs also nest on adjoining sides not visible here. B: scree area scattered with rockfalls, dry vegetation and peat areas. C: peatlands

5

also establish on the sides of the rock formation.

No counting of the total seabird population at Alkhornet was available for this study. However, in 2005, the Norwegian Polar Institute (NPI) assessed the population size on the main wall and in the proximity. This count estimated 13860 breeding pairs of kittiwakes and 13038 – 15212 breeding pairs of Brünnich's guillemots (Strøm, pers. comm. 2018). A counting in 1990 assessed the population to be 11792 kittiwake pairs and 12788-14920 guillemot pairs (Camphuysen & den Ouden 1995). Since 2005, the population trend on Spitsbergen has been stable or slightly decreasing for kittiwakes, and there has been an average annual decrease of 4% in Brünnich's guillemots (Anker-Nilssen *et al.* 2018). This average annual decrease have been similar across all monitored colonies on Svalbard, although different short term fluctuations have been observed among colonies (Descamps *et al.* 2013). Applying a 4% decrease to the 2005 count yields a 2018 estimate of 7669 to 8948 guillemot pairs. In addition, breeding populations of northern fulmars (*Fulmarus glacialis*), Atlantic puffin (*Fratecula arctica*), little auk (*Alle alle*) and glaucous gull (*Larus hyperboreus*) are found in the area, although in much lower numbers (Camphuysen & den Ouden 1995).

Beneath the Alkhornet rock formation, a 500 meters wide plateau stretches out to the coast. This south facing plateau is composed of different marine deposits, metagabbro and limestone. Compared to the general vegetation on Svalbard, the flora is remarkably lush and diverse here, due to the seabird guano fertilisation (Johansen *et al.* 2009). A vegetation gradient is evident with distance from the colony. *Cochlearia groenlandica* is dominating near and on the rock wall. Beneath the rock wall, high guano input combined with the continuous falling of rocks and nest material has led to it being inhospitable for green plants. Instead there is a thick layer of a guano and soil mixture. Further down and towards the coast, mosses, lichen and graminoids like *Festuca rubra, Poa alpine* and *Deschampsia alpina* dominate. A thick layer of peat can be observed in great extent on the flat plateau and in undisturbed hills (Figure 3, section C), measuring up to 1.5 meters in depth (Låg 1990). The productivity here is high and combined with good nutritional value of the plants (*e.g.* low C:N molar ratio), it further supports populations of geese, fox and reindeers (Eide *et al.* 2005; Jakubas *et al.* 2008)

With the Fram strait as its neighbour to the west, the coastline of the study site is highly exposed to weather and ocean forces. In general, the water circulation in Isfjorden is

characterized by Atlantic influenced waters entering the fjord in the south and circulating around the fjord basin before exiting at the north side of the fjord mouth (Nilsen *et al.* 2008), where the study site is located. In the shallow coastal area studied here, wind and waves are important circulation forces, especially at Alkhornet which commonly experiences rough weather. From the coastline, there is a shelf, 2-7 meters deep, continuing 50-150 meters out before it drops to depths of 3-400 meters. The shelf is covered by a rich kelp forest, only fragmented by patches of sand and gravel (pers. obs.). The coastal water mixing at the study site will thus be substantial, likely lessening the impact of terrestrial sources by dilution and water exchange.

2.2 Sampling and analysis

Fieldwork was carried out in the summer of 2018 on five occasions (Table 1). Sampling started just as the snowpack in the creek beds started to thaw in June and ended as the creeks froze or dried out in September.

Table 1: Overview of all samples collected, both in the streams and at the adjacent coast. Study stream B2 was not reached on the 12th of July but was sampled on the 17th of July. In addition to the samples listed here, 3 kittiwake guano samples for Stable Isotope Analysis (SIA) were collected from Alkhornet, 1 in early July and 2 in late July. Amphipods are here listed as number of individuals, these were later pooled after taxa (N=8).

Sample type		Date	B1	B2	B3	C1	C2	C3	Analysis
Study streams	Water	June (14.06)	x	x	x	-	x	x	SIA, TOC, TN, TP, NH_4^+, $NO_2^-+NO_3^-$, PO_4^{3-}, SiO_4, TotHg
		early July (12.07)	x	x	x	x	x	x	
		late July (31.07)	x	x	x	-	x	x	
		August (25.8)	x	x	x	-	x	x	
		September (20.9)	x	x	x	-	x	x	
Algae	Stream periphyton	August	x	x	x	-	x	x	SIA
	Acrosiphonia sp.	August	-	x	x	-	x	x	
	Ectocarpus sp.	August	x	-	-	-	-	-	
Amphipoda	*Gammarus setosus*	August	-	12	8	-	8	13	SIA, MeHg
	Gammarellidae	August	-	3	-	-	4	4	SIA, MeHg
	Caprella sp.	August	-	6	-	-	-	-	MeHg

2.2.1 Stream water sampling and analysis

Stream water was collected in 5 L dark containers, kept cool and brought back to the UNIS lab within 24 hours. Photos were taken of the study streams on all sampling occasions to provide visual documentation of water level and sediment load (Figure 3 for July only, Appendix C for all dates). After returning to the lab, temperature, pH and conductivity of the stream water samples were measured with a multisensor (Hanna instrument HI98196). Turbidity was measured with a Thermo Scientific Eutech TN-100 hand-held turbidity sensor.

Double bagged 250 mL FLPE bottles (trace-metal clean) were filled with sample water, frozen and sent for analysis of the total concentration of all mercury species (TotHg)

(N=26). 100mL plastic containers were filled and fixed with 1 mL 4M sulphuric acid and frozen before analysis of all total phosphorous (TP) (N=26). 100mL amber glass bottles were filled and fixed with 1 mL 4M sulphuric acid for total organic carbon (TOC) and total nitrogen (TN) (N=25, one bottle was lost) and stored at 4 °C. 100 mL sample was filtered through a 0.2 μm pore size membrane and fixed with 1 mL 4M sulphuric acid. These bottles were frozen before being analysed for PO_4^{3-}-P, NH_4^+-N and NO_3^- + NO_2^--N (N=26). The remaining water was filtered onto duplicate pre-combusted glass fibre filters (Whatman GF/F) and frozen at -20 °C for analysis of $\delta^{13}C$ and $\delta^{15}N$ (SIA) (N=52).

TOC and nutrient analyses were carried out at NIVA's analytical lab, using standard and accredited methods (described by (Kaste *et al.* 2018)). See Appendix A for a table summarising all methods. Spectrophotometry was used to find concentrations of TOC, TP, TN, PO_4^{3-}-P and SiO_2. NH_4^+-N and NO_3^- + NO_2^--N was analysed with ion chromatography. For TotHg in water samples, cold vapor atomic fluorescence spectrometry (CVAFS) was used (Braaten *et al.* 2014b). Hg in the sample was oxidised, purged and trapped in a gold trap before analysed in the CVAFS (Olson & DeWild 1997). Analysis was done automatically with a MERX automated system with Model III AFS Detector; Brooks Rand Labs.

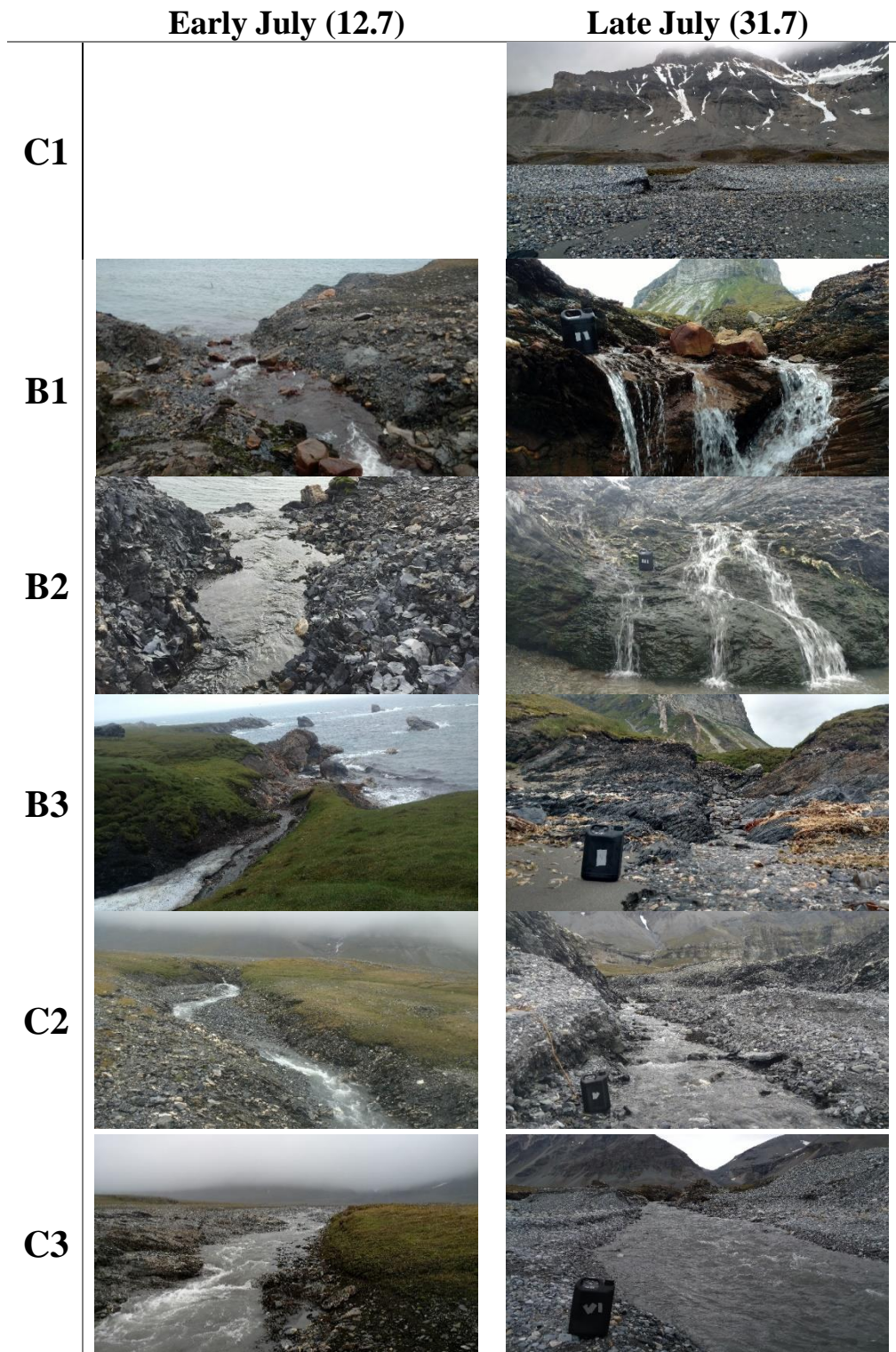|	**Early July (12.7)**	**Late July (31.7)**

Figure 3: Stream stations in July 12th and July 31th. The black containers in the late July pictures is a 5L carboy included for scale. No picture was taken at C1 in early July.

2.2.2 Biota

In August, filamentous epilithic algae were collected from stream station B1-B3 and C2-C3 (Table 1). The samples were added to 75 mL Falcon tubes with stream water and brought back to the UNIS lab within 24h. Here, the algae were rinsed in deionized water and frozen (-20 °C). At the mouth of the study streams, marine sampling was conducted in the littoral zone of the coastline and skerries. The numeration of the marine stations corresponds to the study streams. In addition to study stream C1 being sampled only once, the coast here consists of pebbles and sand exposed to waves and, in the winter, ice scouring. This makes it a different habitat than the limestone formations of the five other stations and it was difficult to obtain comparable taxa for primary producers and consumers. As a result, combined with limitations in time and logistical constraints, station C1 was omitted. The green macroalgae *Acrosiphonia* sp. was collected from tidal zones and, like the freshwater algae, rinsed in deionized water and frozen. As this species was not found at station B1, *Ectocarpus* sp. was collected as a substitute. Amphipods were opportunistically sampled and left for more than 24 hours in 5 µm filtered seawater at 5 °C to clear their guts, then wrapped in aluminium foil and frozen whole.

2.2.3 Stable isotope analysis (SIA)

To trace seabird influence in coastal ecosystems, stable isotopes (SI) of nitrogen ($\delta^{15}N$) and carbon ($\delta^{13}C$) were utilised. Stable isotope analysis (SIA) builds on the principle of Briscoe and Robinson (1925), stating: "In any multiphase system, there is a preferential fractionation of isotopes, with one phase preferentially incorporating the heavy (or light) isotope relative to other coexisting phases."

As metabolic processes is the most important fractionating process of ^{15}N, this isotope is widely used in analysis of trophic position and food webs, with higher $\delta^{15}N$ values in higher trophic level organisms (Peterson & Fry 1987). This trait will have an important role in following the fate of ornithogenic matter, as the influenced coastal ecosystem is expected to have elevated values relative to non-influenced ecosystems. In comparison, carbon does not experience strong isotopic fractionation from one trophic level to the next, and $\delta^{13}C$ can therefore be used to indicate main food sources. On Svalbard, effectively all plants use C3

photosynthesis, which yields low ^{13}C values compared to reference standards. This terrestrial signal will also be different than from marine algae. Different geochemical properties, the type of minerals and their solubility can further result in differences in δ^{13}C in C-containing compounds in runoff, which will be reflected in primary producers.

Samples were prepared for SIA at UiO. All samples were freeze dried in a Leybold-Heraeus GT2 connected to a TRIVAC E vacuum pump. The amphipods, guano and macroalgae were crushed to a homogenous powder and weighed into tin capsules using a Mettler Toledo MX5 Micro balance. In order to remove inorganic carbonates, subsamples of the homogenized amphipods were acidified with 1M HCl (Brodie *et al.* 2011; Søreide & Nygård 2012) and freeze dried again before weighing and encapsulation. Homogenised amphipod samples were further divided into two sub samples, one for SIA and one for MeHg analysis. As two filters were taken from each stream sampling, one in each pair were acidified before freeze drying and packing in tin capsules. The acidification was done to remove inorganic carbonates. Only the acidified filters from July were analysed to reduce analytic cost.

Analysis of δ^{13}C and δ^{15}N was carried out at the UC Davis Stable Isotope Facility with a continuous flow Isotope Ratio Mass Spectrometer. Three references, (bovine liver, glutamic acid and enriched alanine), were provided by UC Davis Stable Isotope Facility. For δ^{15}N and δ^{13}C, the long-term standard deviations were ≤ 0.4 and ≤ 0.2, respectively.

After (Peterson & Fry 1987), the isotope values are presented in the form of:

$$\delta^{15}N \text{ or } \delta^{13}C = \left(\left[R_{sample} - R_{standard}\right] - 1\right) \times 1000,$$

where $R = \dfrac{^{15}N}{^{14}N}$, or $\dfrac{^{13}C}{^{12}C}$

12

2.2.4 Mercury analysis of amphipods

Subsamples of the homogenised amphipods were analysed for MeHg at the Environmental Science and Analytic Chemistry Department of Stockholm University. MeHg was extracted through digestion with nitric acid, ethylated and analysed with a 2700 Methyl Mercury Auto-Analysis System (Braaten *et al.* 2014a; Hintelmann & Nguyen 2005). Briefly, the mercury is purged with nitrogen, trapped and analysed with cold vapor atomic fluorescence spectrometry (CVAFS).

2.3 Data processing and statistical analysis

2.3.1 Characterisation of stream catchments and runoff

NPI's Digital Elevation Model (DEM) with a ground pixel size of 5x5 metres was used for delineation of catchment area. A drainage direction raster was made with GRASS GIS tools (GRASS Development Team 2017; QGIS Development Team 2019) and from this; the catchment draining towards the coordinates of each station was delineated (Table 2). In addition, the distance between sampling site and the centre of the colony on the Alkhornet rock wall was measured in QGIS.

Table 2: Attributes of stream catchments, their areal and distance from the colony centre to the sampling point for each station

Stream station	Catchment area (km^2)	Distance from colony (km)
Station B1	0.24	0.77
Station B2	0.14	0.75
Station B3	0.22	0.79
Station C1	0.30	1.83
Station C2	0.73	2.19
Station C3	3.74	3.41

Discharge was not measured, but an approximation can be made from meteorological data and estimation of the water budget (Poncea & Shetty 1995). As 1 mm of water equals 1 L per m^2, having both the catchment size and estimation of surface runoff yields the stream discharge. Except for station C3, no glaciers are found in the catchment basins and the sources of surface runoff would be limited to precipitation and melting of snow and ice.

The annual water balance of a catchment can be referred to as (Poncea & Shetty 1995);

$$P_A - Q_S - Q_G - E_A \pm \Delta M = \varepsilon \,,$$

where P_A is the precipitation input, Q_S is the surface runoff, Q_G is the ground water runoff, E_A covers evaporation and transpiration, ΔM is the change in water budget and ε is an error term. Previous work from Svalbard (Killingtveit *et al.* 2003) recorded a yearly precipitation of 595 mm and 411 mm surface runoff for the London river at Svalbard. With the lack of glaciers in the catchments, ΔM can be assumed to be zero when calculating the yearly water budget. Hence, 69% of the annual precipitation ended up as surface runoff in London river. This river runs on the peninsula Blomstrandhalvøya and is comparable to the Alkhornet streams; the catchment basin is 0.7 km^2, it is glacier free and the precipitation regime is similar in both locations.

To make estimations on runoff based on weather data, daily recordings of precipitation and temperature data, starting in November 2017, were downloaded from the Norwegian Meteorological Institute (eklima, http://sharki.oslo.dnmi.no/, accessed January 2019). These data are observations from the weather station at Isfjord radio, about 15 km south of the study area. The temperature is measured continuously, and the daily mean was used. Recordings from the 5th and 12th of July are missing, and these days are therefore omitted in the further use. Precipitation is recorded at 07:00 am, and therefore reflects the previous night and day. Additional precipitation data were obtained from the AROME Arctic weather model. The model assigns a value to grid cells with 2x2 km size, and a median of a cell matrix with 3x3 cells around Alkhornet was used. Isfjord radio recorded a total of 190 mm precipitation in the sampling period, from 14.06-20.09. From 1.11.2017-13.06.2018, 221 mm precipitation was recorded. AROME predicted 274 mm and 421 mm, respectively.

Given the same surface runoff to precipitation relationship as in London river (0.69), the yearly runoff based on the Isfjord radio data should equal 284 mm and based on AROME; 479 mm. The mean of the precipitation three days prior to sampling was used for the

14

influence of rain events. The August and September precipitation means were scaled by 0.69 and the June and early July scaled up to account for snowmelt. The precipitation average for June was multiplied with 3.5 and early July multiplied by 1.7. This made the area under curve (AUC) integrate to a yearly runoff of 284 and 479 mm in the Isfjord radio and AROME scenarios respectively. All numbers are summarised in table 3, see Appendix B for graph comparing the two runoff scenarios with the precipitation and temperature data for the whole sampling period.

Table 3: Summary of 3-day precipitation means and derived runoff estimates for Isfjord radio measurements and AROME model data. The AUC for the different precipitation and runoff scenarios, integrated over the whole sampling period, is also listed.

Sample date	Precip. mean, Isfjord radio (mm)	Precip. mean, AROME (mm)	Estimated runoff, Isfjord radio (mm)	Estimated runoff, AROME (mm)
June 14th	0.63	0.44	2.13	1.54
July 12th	4.37	7.99	7.35	14.1
July 31th	1.60	3.41	1.60	3.41
August 28th	0.73	0.12	0.50	0.08
September 20th	1.03	0.001	0.71	0.001
June-September (from AUC)	192	295	284	479

Having estimated the runoff in mm per sampling day, this was converted to m^3/day by scaling to catchment sizes. The nitrogen yield for the whole season at the different streams was then numerically integrated, using the AUC function in the R package MESS (Ekstrøm, C. 2011) with the spline function (Yeh & Kwan 1978).

2.3.2 Bioenergetics

The annual mass of guano deposited was estimated by the bioenergetics model and parameters used in previous studies (Otero *et al.* 2018; Riddick *et al.* 2012; Wilson *et al.* 2004):

$$N_{excr(adult)} = \frac{9.2M^{0.774}}{F_{Ec}A_{eff}} F_{Nc} t_{breeding} f_{tc} \tag{i}$$

$$N_{excr(chick)} = \frac{28.43M_{fledging}^{1.06}}{F_{Ec}A_{eff}} F_{Nc} \frac{P_{chick}}{2} \tag{ii}$$

The total mass of nitrogen excreted in the breeding colony by adults and chicks is estimated as the excretion from breeding adults, non-breeders and chicks. Annual deposition from one breeding adult are here equal to the field metabolic rate (FMR) (kJ d^{-1}) divided by the wet weight energy density of the food (kJ g^{-1} w.w., F_{EC}) and the ratio of energy obtained from the food (A_{eff}), times the N content in the food (F_{NC}). Body mass is used to calculate FMR, as the FMR is highly dependant on the mass of seabirds (Dunn *et al.* 2018). Furthermore, the deposition is scaled to the amount of days in the colony ($t_{breeding}$), and the proportion of time spent in the colony ($f_{tc(br)}$). For non-breeders, equation (i) is used as well, but $f_{tc(br)}$ is exchanged for $f_{tc(nbr)}$, accounting for the low number of non-breeding birds and shorter colony presence. Non-breeders are here expected to make up 1/3 of the population and spending 1/2 as much the time in the colony as breeders. In (ii), the nominator estimates energy requirements for growth to the mass of the fledging chicks ($M_{fledging}$) and is thus one value for the whole brooding period. P_{chicks} is the expected productivity per breeding pair, defined as the expected number of chicks fledged per pair per season. The calculations were performed for the Brünnich's guillemots and Black-legged kittiwakes at Alkhornet (see Table 4 for values used).

Table 4: Parameters included in the estimation of N-deposition at Alkhornet, taken from [a]Strøm, pers. comm (2018), [b]Barrett et al. (2002), [c]Wilson et al. (2004).

	Breeding pairs	Mass, adult (g)	Mass, fledgling (g)	F_{EC} (kJ/g w.w.)	A_{eff}	F_{Nc} (w.w.)	$t_{breeding}$ (d)	$f_{tc(br)}$	$f_{tc(nbr)}$	P_{ch}
U. lomvia	7669[a]	998[b]	212[c]	5.4[b]	0.8[c]	0.036[c]	70[b]	0.6[c]	0.1[c]	0.74[c]
R. tridactyla	13860[a]	409[b]	320[c]	5.7[b]	0.8[c]	0.036[c]	90[b]	0.6[c]	0.1[c]	0.78[c]

2.3.3 Estimation of normalised difference vegetation index (NDVI)

The normalised difference vegetation index (NDVI) was used as a measure of seabird influence on the terrestrial vegetation. This index is calculated as follows;

$$NDVI = \frac{NIR - red}{NIR + red}$$

where NIR is near infrared spectral bands (700-805 nm) and red is red bands (635-675 nm).

Photosynthetic plants absorb light in the red spectre, but have high reflectance of NIR light, and will have positive NDVI values. Bare soil and rocks will have similar albedo for NIR and red light, while snow will have higher albedo for NIR than red light and have negative NDVI values (Carlson & Ripley 1997). Previous work have related different vegetation types with NDVI values on Svalbard (Johansen *et al.* 2009) and vegetation close to bird cliffs have among the highest measured values.

Norwegian Polar Institute (NPI) provided an 8-bit aerial orthophoto from 2009 with a ground pixel size of 0.4x0.4 metre and taken with an UltraCam X sensor. NDVI calculation were done with the i.vi. tool in the QGIS GRASS package (GRASS Development Team 2017; QGIS Development Team 2019). To lessen the noise introduced by the sensor, a gaussian smoothing operator was used. Each pixel was recalculated to fit within 1 standard deviation of a matrix compromising a radius of 3 cells around the central cell. Due to the large size of the datasets, 10 000 cells were randomly sampled from each catchment. Medians and density functions were calculated from these subsets. In C3, a distortion in the waveband was detected in the top left corner of the catchment, giving rise to unreasonably high NDVI. This corner was therefore excluded in the calculation of NDVI median.

2.3.4 Ordination and statistical exploration

To get an overview of all measured parameters and how well the *a priori* grouping of seabird influenced streams and reference streams were reflected in the data, a principal component analysis (PCA) was carried out. PCA can be considered a type of ordination, which approximate all variation in the multivariate dataset to a set of new dimensions, explaining successively less variation. PCA uses Euclidian distance as a measure of dissimilarity, and adds variables by linear regression (Greenacre & Primicerio 2014). The dimension explaining most of the variation is referred to as the principal component 1 (PC1) and the uncorrelated dimension explaining the second most variance as PC2 (Greenacre & Primicerio 2014). The PCA was performed on a matrix of TN, TP, $NO_3^-+NO_2^-$, PO_4^{3-}, SiO_2, NH_4^+, TOC, TotHg, $\delta^{15}N$, $\delta^{13}C$, and particulate C and N (partC, partN) values for all sampling dates and sites. All parameters were standardised to a mean of 0 and standard deviation of 1.

Subsequently, a subset of the parameters was selected to avoid missing values and to reduce the dependence between parameters due to their intrinsic properties, i.e. between TN and $NO_3^-+NO_2^-$. This subset contained 8 variables; TP, $NO_3^-+NO_2^-$, SiO_2, $\delta^{15}N$, TotHg, $\delta^{13}C$, partC and partN. To explain causes of variation in the matrix, the following environmental variables were passively fitted to the ordination; turbidity, catchment size, NDVI medians of the catchments, runoff estimates, precipitation estimates, sample date, air temperature and distance to centre of the colony. A redundancy analysis (RDA) were performed on each environmental variable, where the 8 selected parameters were used as response variables. A permutation test with 100,000 permutations was then used on the RDA to test for the explanatory contribution of the environmental variables. Variables with p-values above 0.05 were discarded in the final ordination diagram.

Variance partitioning was further used to investigate the explanatory contribution of each environmental variable on the 8 selected parameters. A best model was built with forward selection from a null model. Starting with the environmental variable with the highest "pseudo-F" from the permutation test of the RDA, this variable was constrained while a second one was added. The added variable contributing to the largest increase in variance explained according to the pseudo-F was retained, given it was significant (p<0.05). These two variables were then constrained, and a third variable was added, and so on. The process terminated when adding the next variable did not result in a significant increase in variance explained.

18

3 Results

3.1 Stream characteristics

The streams showed different characteristics both in the overall concentrations of different compounds and in seasonality. The difference in seasonality is reflected in the turbidity (Table 4). Initially, turbidity was low in all streams, but the control stations C2 and C3 had high sediment load in July. Throughout the season, B2 and B3 remained low, while the particle load increased in B1. The same pattern can be seen in $\delta^{13}C$ values, where the turbidity increase in the control stations was due to more inorganic particles, seen as an increase in the unacidified $\delta^{13}C$ values (Figure 4).

The difference between streams was particularly apparent in the $\delta^{15}N$ values, which were consistently 5-10 ‰ higher in bird influenced streams relative to the controls (Figure 4). In addition to higher $\delta^{15}N$ values, concentrations of NH_4^+, $NO_3^- + NO_2^-$, PO_4^{3-} and TOC were all higher in the seabird streams than the control streams (Welch t-test, all with $p<0.05$) (Figure 4).

Table 5: Stream pH and turbidity. September was not measured. Turbidity is given as mean of three measurements ± 1 standard deviation.

	Turbidity				pH			
St.	June	July, early	July, late	August	June	July, early	July, late	August
B1	1.1 ± 0.1	11.0 ± 0.5	10.1± 0.2	59.7± 2.3	7.9	8.0	7.7	7.1
B2	3.4 ± 0.3	1.4 ± 0.2	0.6 ± 0.1	1.0 ± 0.5	8.0	7.6	8.0	7.8
B3	1.2 ± 0.2	4.2 ± 0.9	0.8 ± 0.0	0.8 ± 0.3	7.9	7.8	7.8	7.6
C1	-	1.1 ± 0.3	-	-	-	7.7	-	-
C2	1.0 ± 0.1	15.2 ± 1.4	0.7 ± 0.2	0.7 ± 0.3	8.2	7.8	7.9	7.9
C3	1.0 ± 0.4	41.1 ± 2.0	29.1 ± 0.8	2.8 ± 0.4	8.1	8.0	7.5	7.8

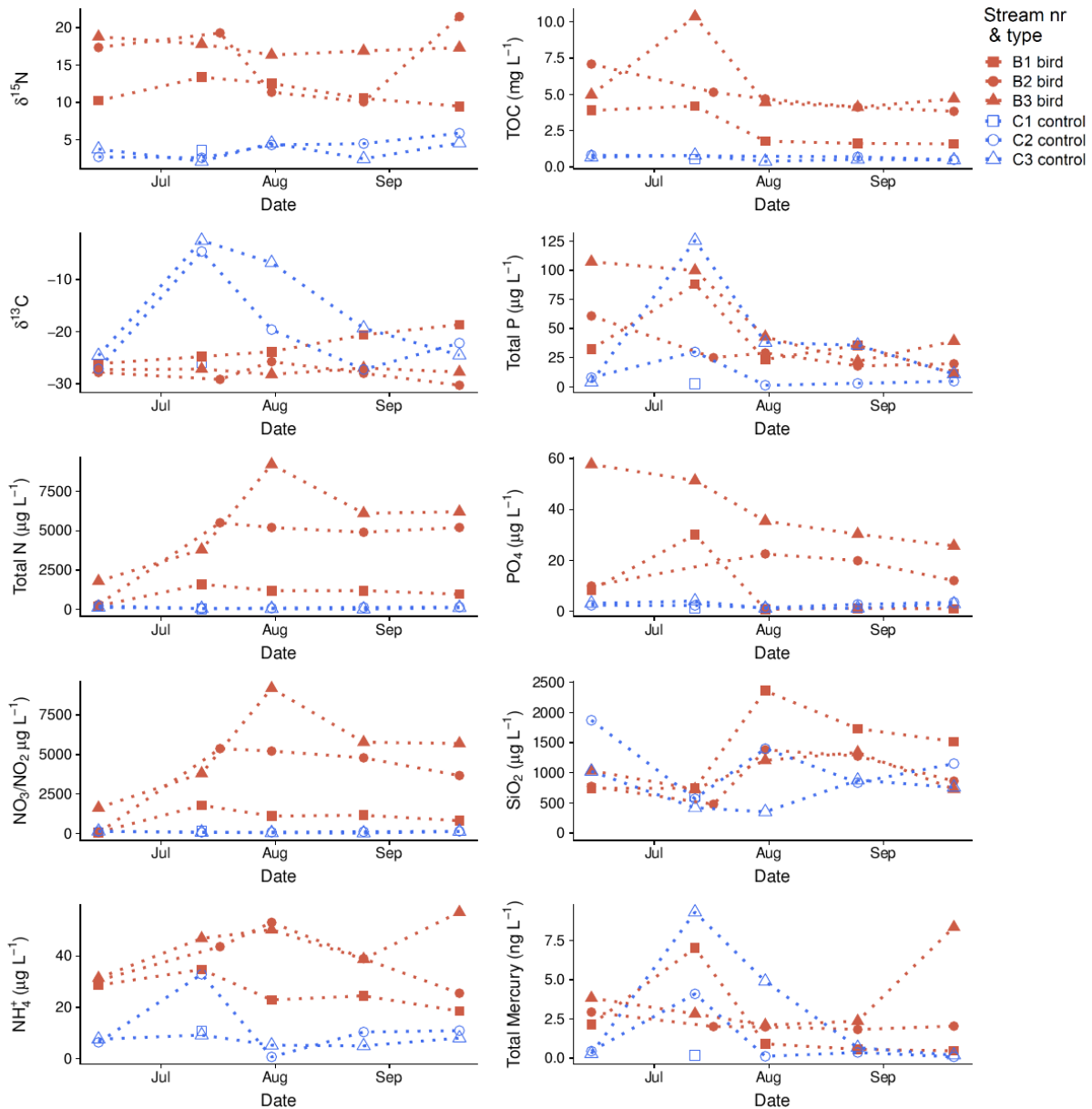Figure 4: Seasonal change in particulate isotope ratios (δ^{15}N and δ^{13}C) and water chemistry parameters for the 6 study streams. Red colour indicates bird influenced streams and blue indicates controls, and the different symbols corresponds to stream numeration.

Station C2 had a TOC concentration of 19 mg/L on the 31st of July. This outlier was removed as the turbidity, water colour and the rest of the TOC values for control streams made such a high value unlikely. A clear difference in seasonality of TotHg in bird and control streams emerge. While the three seabird influenced streams have rather stable TotHg concentrations of ~3 ng/L, the control streams display seasonality with lower values (0.06-0.63 ng/L) in June, August and September and some higher values in July (0.11-9.3 ng/L). Turbidity was the best predictor for TotHg concentrations in control streams, while TOC was the best

predictor for TotHg in bird streams. The opposite combinations performed poorly (Figure 5). While both control and bird streams had similar TP concentrations, PO_4^{3-} was only a large contributor to TP in bird streams, leading to a poor correlation of 0.3 between these parameters (Appendix D). Similarly to TotHg, TOC and turbidity was used to predict the TP values in the streams and the same pattern was observed, with TP associated with TOC in bird streams, and with turbidity in control streams (Appendix E).
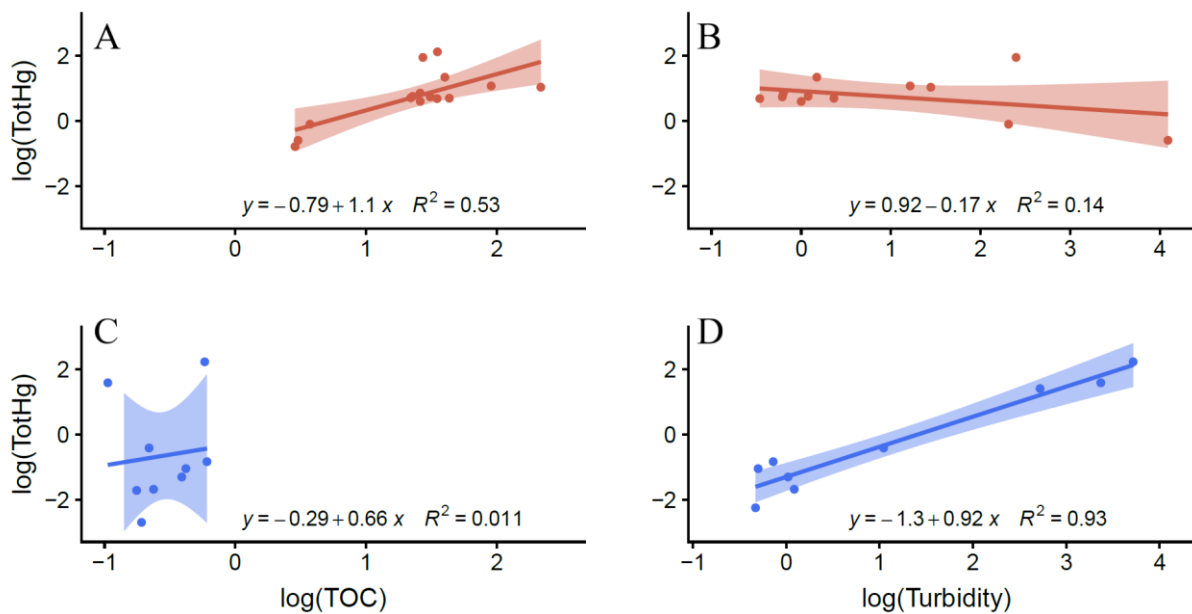

Figure 5: Regression of TotHg in streams predicted by TOC and turbidity for bird influenced streams (red, A-B) and control streams (blue, C-D). All variables are log transformed to achieve a normal distribution (Shapiro-Wilk normality test, all variables with $p < 0.01$). See Figure 4 for untransformed values.

3.2 Biota

δ^{15}N values were found to be higher in biota from seabird influenced sites for all taxa analysed (Figure 6). The discrepancy in δ^{15}N was larger for the stream periphyton and marine macroalgae than for the amphipods, but the differences in δ^{15}N between control and seabird influenced sites were statistically significant for all three sample types (Welch t-test, p-values of 0.026, 0.016 and 0.0003 respectively).
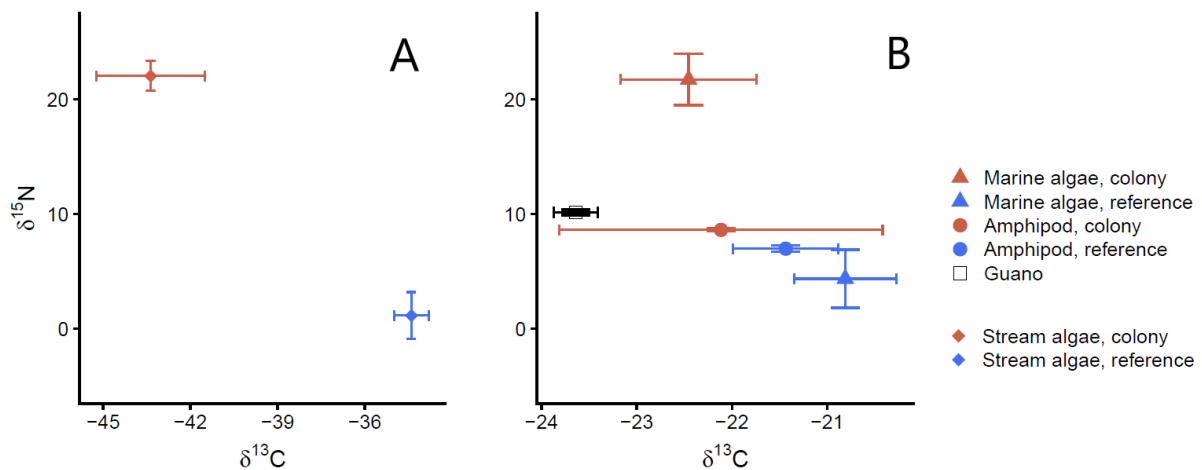

Figure 6: Stable isotope biplot for biota. A) shows the values of stream periphyton (N=3 for seabird influenced and N=2 for reference) and B) displays *Acrosiphonia* sp. (N=3 for seabird influenced and N=2 for reference), marine amphipods (N= 3 for seabird, and N= 4 for reference and kittwake guano (N=3). Amphipod δ^{13}C values are from acid treated samples, and δ^{15}N values non-acidified. All error bars are equal to 1 SD.

Acrosiphonia sp. sampled at B2 and B3 had an atomic C:N ratio of 10.4:1 and 11.3:1 respectively, while the controls C2 and C3 had 14.0:1 and 14.7:1 (Welch t-test, t = -6.3, p-value = 0.029). The epilithic stream periphyton from stations B1, B2 and B3 had C:N ratios of 10.0:1, 10.4 and 11.0:1, while the controls had 8.9:1 and 8.2:1 (Welch t-test, t = 2.3, p-value = 0.111). However, the species in these stream communities were not identified and could give rise to the variability observed.

Contrary to our hypothesis, amphipods had higher MeHg values at the control sites than at the bird station (Welch t-test, t = 3.5, p=0.017) (Table 6). No correlation was found between amphipod size or taxa and MeHg concentration.

Table 6: Overview of the amphipods pooled for MeHg analysis. The MeHg concentration is given as ng/g dry weight, together with the number and mean weight of amphipod individuals are included. All samples were collected in August.

Station	Species	MeHg (ng/g)	Individuals	Mean weight (g)
B2	*Gammarus setosus*	0.4257	12	0.095
B3	*Gammarus setosus*	1.761	8	0.39
B2	Gammarellidae	2.709	3	0.14
C2	*Gammarus setosus*	5.799	8	0.075
C3	*Gammarus setosus*	6.325	13	0.036
C2	Gammarellidae	3.909	4	0.16
C3	Gammarellidae	5.054	4	0.050
C3	*Caprella* sp.	2.944	6	0.11

3.3 Quantifying the flux

Based on the bioenergetics model, the seasonal nitrogen deposition in the colony was estimated to be 675 g per breeding *U. lomvia* individual and 410 g per breeding *R. tridactyla*. In addition, contribution from non-breeders and chicks per breeding individual were estimated to be 113g and 26 g nitrogen respectively for *U. lomvia* and 68g and 40 g nitrogen for *R. tridactyla.* This adds up to 27 895 kg nitrogen for the whole colony, where *U. lomvia* contributes with 13 517kg and *R. tridactyla* with 14 378 kg.

As expected, the total mass flux of TN was predicted to be higher in the bird streams than in the controls (Table 7), despite the higher discharge in the controls. While C3, and to some extent C2, discharge large amounts of phosphorous, only a small fraction is present as PO_4^{3-} compared to the bird streams (Table 7).

Table 7: Estimates of nitrogen, phosphorus (TP and PO$_4^{3-}$-P), TOC and TotHg fluxes from the study streams interpolated for the whole season. These are given as both total mass fluxes and areal fluxes. The two values are derived from the two runoff scenarios, where the low estimates are based on precipitation measured at Isfjord radio and the high is from the AROME weather model predictions. There are no flux estimates for C1 due to only one sampling date, and no TOC flux estimates for C2 due to the two NA values.

Station	TN flux (kg)	TN areal flux (g/m²)	TP flux (kg)	TP areal flux (g/m²)	PO$_4^{3-}$ flux (kg)	PO$_4^{3-}$ areal flux (g/m²)	TOC flux (kg)	TOC areal flux (g/m²)	Hg flux (g)	Hg areal flux (µg/m²)
B1	97 – 170	0.4 – 0.7	14 – 27	0.061-0.11	4.7 – 8.9	0.020-0.036	0.76 – 1.3	0.0032-0.0055	1.1 – 2.1	4.7 - 8.7
B2	190 – 360	1.3 – 2.5	3.7 – 6.0	0.025-0.038	1.8 – 2.8	0.015-0.027	0.65 – 1.1	0.0045-0.0075	0.3 – 0.4	1.8 - 2.9
B3	270 – 470	1.2 – 2.1	17 – 29	0.076-0.13	9.1 – 16	0.041-0.071	1.6 – 3.0	0.0075-0.013	0.6 – 0.9	2.5 – 3.9
C1	–	–	–	–	–	–	-	-	–	–
C2	19 – 27	0.026-0.037	14 – 26	0.020-0.036	1.4 – 2.3	0.0019-0.0031	-	-	1.9 – 3.6	2.6 – 4.9
C3	69 – 110	0.018-0.029	310 – 590	0.083-0.16	11 – 19	0.0029-0.0051	2.3 - 3.9	0.00061-0.001	24 – 45	6.3 - 12

3.4 Normalised Difference Vegetation Index

The median NDVI was close to 0 in the three control catchments and around 0.3 in the bird catchments (Figure 7 and Appendix F). The seabird influenced catchments contain highly variable vegetation from wet peat and marshland to dry meadows, with rockfalls close to the mountain. This gave rise to larger variation in NDVI here than in the control catchments (Appendix F). The area with consistently higher NDVI values than 0.3 covers about 1.8 km^2 on Alkhornet (Appendix F). Combined, the B1, B2 and B3 catchments covers 0.6 km^2 of this area.
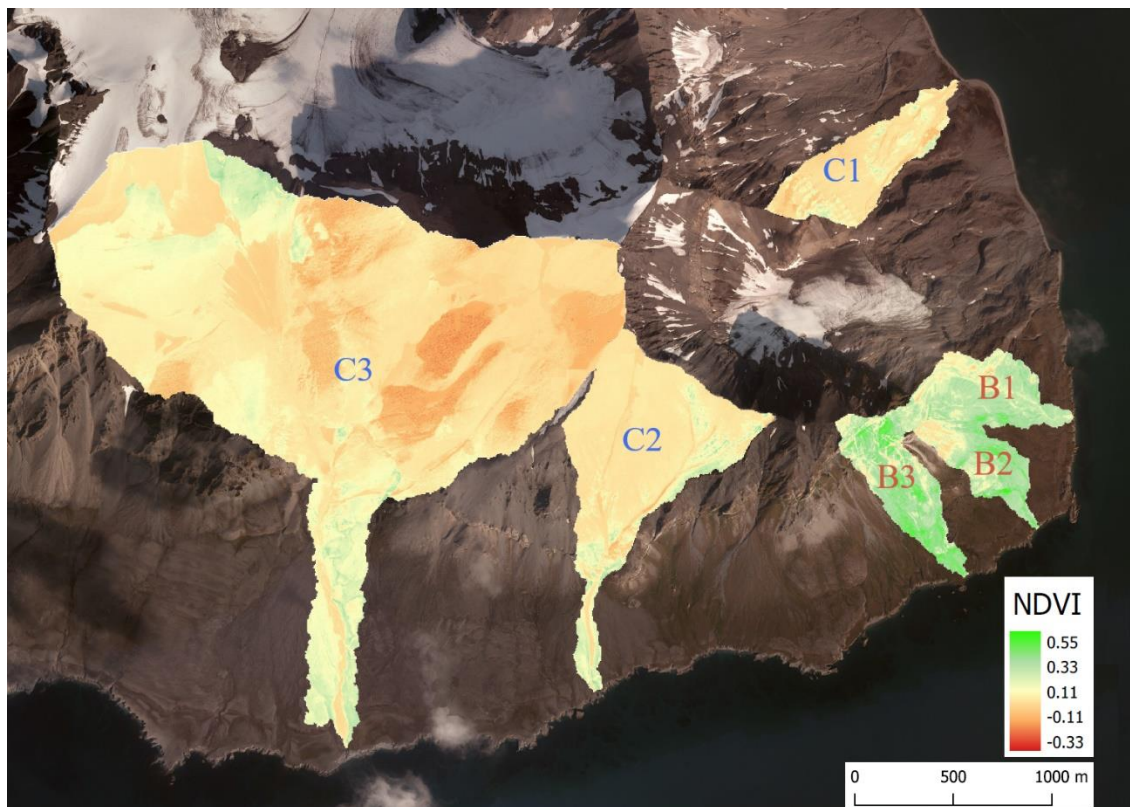
Figure 7: Heatmap of NDVI values in in the 6 stream catchments investigated. Median values were as follows: C1: 0.0357, C2: 0.0504, C3: 0.0353, B1: 0.260, B2: 0.290, B3: 0.324

3.5 Exploration of stream parameters

The variance in stream parameters is summarised in the PCA ordination diagram (Figure 8). Sampling dates scatter along the first axis (PC1) within each station. The sampling in early July stands out as the most different, having the most positive PC1 values for all stations except B2, which was sampled almost one week later. Early July was also when the discharge was largest, and both the runoff variable and sample dates are associated with this axis. The second pronounced trend is the separation of stations along the second axis (PC2), B2 and B3 group together on the negative side and C1, C2, C3 group on the positive side. B1 is placed in the centroid and between these two groups. Median NDVI in the catchment, runoff and catchment size were the best environmental predictors (permutation test of RDA, pseudo-F = 7.8, p-value = $6e^{-5}$, pseudo-F = 4.6, p-value = 0.005 and pseudo-F = 3.5, p-value = 0.01 respectively). The variance partitioning resulted in an adjusted R^2 of 0.21 for median NDVI, 0.19 for runoff and 0.07 for catchment size. Adjusted R^2 for the three variables combined was 0.43.
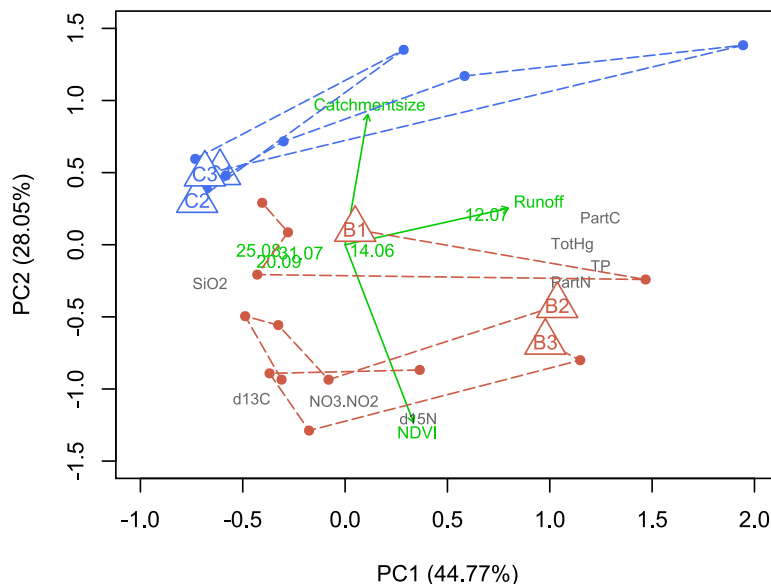

Figure 8: Principal component analysis (PCA) ordination diagram of SiO_2, SI, $NO_3^- + NO_2^-$, TP, TotHg, PartC and PartN. The triangles with station name shows the position for the first sampling date (June) and the proceeding sample dates follow the dashed line. C1 have only one sampling date (early July). Catchment size, NDVI median, runoff estimate based on Isfjord radio weather data and sample date were passively fitted as environmental predictors. The sampling of B2 on July 17th was changed to July 12th in the sample date variable.

4 Discussion

4.1 From sea to land: Estimating seabird nitrogen input and terrestrial retention

Seabird colonies are important point sources of nitrogen and phosphorous on Svalbard, especially when considering the low input from other sources. The nitrogen deposition in the Alkhornet mixed-colony was estimated to be nearly 30 tons in 2018, in congruence with other similar sized bird colonies (Graham *et al.* 2018; Otero *et al.* 2018) when accounting for the different body size of bird species and time spent in the colony. This estimate has a high degree of uncertainty, since several assumptions were made on the parameters included in the bioenergetic models, including population size, time spent in the colony, breeding success, metabolic rates, nitrogen content of the food, assimilation and excretion relationships. The number of breeding pairs can also vary over the breading season depending on chick rearing success. Nonetheless, it highlights the role of the seabird colony as a nutrient point source. Areal differences in seabird activity and number of flyovers together with nutrient dispersal processes will create a gradient of decreasing seabird influence when moving away from the colony. Thus, defining a border of seabird influence on land is problematic. Here, the nitrogen input was averaged over the area of seabird manured vegetation, defined by NDVI values, at 17 g N m^{-2} y^{-1}. Only a limited number of previous studies have tried to quantify ornithogenic nitrogen deposition, and different geography and species makes comparison difficult. However, values from 5 g m^{-2} y^{-1} (Leblans *et al.* 2014) to 29 g m^{-2} y^{-1} (Breuning-Madsen *et al.* 2010; Leblans *et al.* 2014) have been reported.

Both the NDVI values from bird catchments and controls calculated here are well in accordance with previous assessments on vegetation types for the entire Svalbard (Johansen *et al.* 2009). Furthermore, a positive relationship between phytomass and NDVI is established for Svalbard (Johansen & Tømmervik 2014). With the small geographical scale of the present study, NDVI can be a good indicator of terrestrial productivity, driven by the manurial effect of the colony. Assuming the 1.8km^2 outlined area of seabird influence has similar N-leaching rates as the surveyed streams, the seasonal discharge is about 5-10% of the total nitrogen deposited from the colony by seabirds. Although some nitrogen will be lost through volatilization of NH$_3$, the atmospheric half-life of NH$_3$ can be very short and much will be

redeposited close to the N point source (Pitcairn *et al.* 2002). Furthermore, mosses are highly important in the terrestrial nitrogen retention (Turetsky 2003), and able to retain virtually all added nitrogen in low N-input Arctic tundra (Yano *et al.* 2010). This important sink is highlighted on Alkhornet by the thick peat layer (Låg 1990). However, in a high-input area such as this, we anticipate some nitrogen leaching from decomposition processes and oversaturation.

The accuracy of the estimated nitrogen fluxes in the study streams is dependent on the hydrology data used. Total precipitation in the sampling period estimated from integration of the three-day averages was representative for the sum of all daily values (+1% for Isfjord radio data and -4% for AROME data). Isfjord radio usually underestimate the true precipitation during winter (Førland & Hanssen-Bauer 2000). In addition, this weather station is at sea level, but precipitation can increase substantially with elevation (Killingtveit *et al.* 2003). The AROME weather model accounts for elevation increase, which is one of the reasons why it tends to have higher predictions than the measurements from the weather station. The contribution of snowmelt, precipitation and evapotranspiration to surface runoff was not measured specifically for this study, but based on previous reports from London river (Killingtveit *et al.* 2003). The groundwater transport was assumed to be negligible as it can only occur in the active layer above the permafrost. Finally, the runoff estimates were not verified with other catchments on Svalbard, as the Norwegian water resources and energy directorate (NVE) had no adequate measurements of waterflow for the 2018 season (Songe, pers. comm. 2019). Therefore, these results should be interpreted as a rough estimate on seasonal yield from runoff, where the calculations from Isfjord radio data is a low estimate, and AROME a high estimate.

4.2   From land to sea: Stream water-chemistry

Our first hypothesis, proposing stream closeness to the colony to be associated with high concentrations of TOC, PO_4^{3-}, NO_3^- and NH_4^+, is well supported. The concentrations were consistently one to two orders of magnitude higher in the seabird influenced streams than in the controls. For comparative purposes, it can be mentioned that both the nitrogen concentration in surface runoff and annual nitrogen fluxes is similar to observations from

small agriculturally-influenced catchments in mainland Norway (Bechmann 2014). The dominant form of nitrogen was $NO_3^- + NO_2^-$, as NH_4^+ is readily oxidised in these environments (Banerjee & Siciliano 2012) or assimilated by vegetation (Yano *et al.* 2010). PO_4^{3-} was the dominant form of TP in the seabird influenced streams. In comparison, PO_4^{3-} was only a minor contributor to the TP concentrations in control streams. The TP concentration in control streams was found to be associated with turbidity, suggesting most of the discharged P from these streams are in particulate and geochemical forms (e.g. calcium, iron or aluminium bound-P). These forms are much less available for uptake by primary producers than PO_4^{3-} (Reynolds & Davies 2001).

The importance of seabirds in the nitrogen transport from Alkhornet to adjacent coastal waters is further supported by $\delta^{15}N$ stable isotope data. Seabirds occupy a high trophic position and are recognised to have high $\delta^{15}N$ values. Here, the kittiwake guano had $\delta^{15}N$ values of over 10‰, in congruence with previous work (Wainright *et al.* 1998). Wainright *et al.* (1998) further described guano to have depleted ^{15}N content relative to the bird's blood with -0.7‰ – -4.3‰, meaning the actual trophic position is higher than suggested by the guano. In this study, higher $\delta^{15}N$ was found in particulate organic matter (POM) from the seabird influenced streams, especially at station B2 and B3. The $\delta^{15}N$ values POM from these streams reached 20‰, so it is evident that further fractioning has occurred in the deposited nitrogen. Isotopic fractioning during NH_3 volatilisation from the guano will enrich ^{15}N content of residual nitrogen (Frank *et al.* 2004). The nitrogen isotopes can be further fractioned in microbial processes *e.g.* nitrification and denitrification, and after assimilation by autotrophs. Previous work on the nitrogen flux through Arctic tundra has shown how efficiently nitrogen is assimilated by vegetation, and that most of the N losses through leaching are due to decomposition of organic matter (Yano *et al.* 2010). The role of soil as a transition step between seabird deposition and release to aquatic ecosystems have been observed in other systems as well (Harding *et al.* 2004). Although the $\delta^{15}N$ values in the streams were taken from particulate matter, the dissolved nitrogen in the bird influenced streams is likely similarly high, as evidence by the extremely high $\delta^{15}N$ in epilithic stream algae relative to the $\delta^{15}N$ values for guano. This is due to dissolved inorganic nitrogen being the main available N-source for these primary producers (Dodds *et al.* 2002).

The second hypothesis stated that there should be a seasonal change in stream water chemistry. Concentration of the dissolved inorganic nitrogen in bird streams peaked in

August, while PO_4^{3-} peaked in June and early July. In June, stream discharge (with the exception of B3 where melting had progressed a bit further) was mainly fuelled by snowmelt running through the snowpack. Compared to the later sampling, the amount of $NO_3^-+NO_2^-$ was low (21% of TN in B1 and 6% in B2), while NH_4^+ levels were high (13% of TN in B1 and 10% in B2). This pattern is in congruence with NH_4^+ originating from snow deposited NH_3, while $NO_3^-+NO_2^-$ concentrations only increase when the vegetation and soil thaws. Melting of the soil have been showed to be important in mobilizing NO_3^- in Arctic tundra (Yano *et al.* 2010). The deposition from the colony will cease in August when the birds leave, but nitrogen transport through the soil infer a lag time.

For $\delta^{13}C$, station C2 and C3 display high values corresponding with the highest observed streamflow and sedimentation on the filter. The bedrock in the catchment consist of calcareous phyllite and carbonate (Dallmann 2002), and the large amount of inorganic carbon collected on the filter can explain the high $\delta^{13}C$ values (Brodie *et al.* 2011). This is supported by the acidified filters from controls in June and late July having much lower values than untreated filters (10‰ lower). However, the effect was variable and suggested incomplete acidification.

An interesting separation in total mercury concentrations between bird and control streams was found at a seasonal scale. Levels were initially higher in the seabird streams, but as the season proceeded and the sediment load in the control streams increased, TotHg concentrations also increased. Investigation of the main driver of the mercury concentration highlight the suspended particulate matter, measured as turbidity, as the most important predictor in control catchment. In comparison, the mercury in bird influenced catchments is linked to organic matter, measured as TOC concentrations. Arctic terrestrial vegetation has been showed to be an important sink for mercury (Shotyk 2017). Thus, the thick peat layer on Alkhornet will accumulate much of the mercury input, potentially cancelling out the effect of extra mercury added by seabird deposition. In fact, the areal mercury leaching was similar in both seabird influenced and control catchments with the largest yield reported from C3.

The ordination and variance partitioning suggest that NDVI is the best predictor of the difference between study streams and streamflow to best explain seasonal variance. Among the bird streams, B2 and B3 clusters together in the ordination diagram while B1 is suggested to be more similar to the control streams. A stretch of the moraine south of the glacier Alkhornsbreen can be seen in the catchment of B1, which is likely the cause of this pattern.

30

The amount of runoff is important in explaining the structure of the stream dataset. SiO_2, TotHg, turbidity and TP are all parameters shown to be strongly associated with streamflow. Except for the concentration of SiO_2, which to a large degree is determined by the dissolution and erosion rate, all these parameters were positively correlated with increased runoff.

4.3 Seabird influence on the coastal ecosystem

Our third hypothesis was that the seabird influence would be detectable in the nearby coastal ecosystem. The higher $\delta^{15}N$ values observed for biota from the seabird influenced coastal sites supports the hypothesis that coastal organisms utilise the nutrients discharged from the colony. The $\delta^{15}N$ values of *Acrosiphonia* sp. found at the control sites are in congruence with previous reported data from Svalbard (*e.g.* Sokołowski *et al.* 2014), while the ^{15}N enrichment found at the bird stations implies an substantial ornithogenic nitrogen input to the coast. Seeing an ornithogenic signal despite the large nutrient sink in the terrestrial vegetation and the exposed coastline highlights the importance of seabird colonies as nutrient point sources.

The $\delta^{15}N$ values of the amphipods also differed between seabird stations and controls, but within the range of values reported from a parallel work on Svalbard (Skogsberg 2019). An isotopic signal usually becomes less clear with higher trophic levels as food sources and movement patterns become more complex. The amphipods collected here can display highly variable and opportunistic feeding ecology (Legeżyńska *et al.* 2012). Different strategies such as phytodetrivory, scavenging and deposit feeding will influence their trophic position and exposure to ornithogenic influence. Furthermore seasonality can greatly affect $\delta^{15}N$ values (Skogsberg 2019). However, the minimal variance within the values from both seabird influenced and control stations, combined with the apparent similarity of habitat, lend support to a possible seabird signal in amphipods from influenced sites.

Although the stable isotope data suggest assimilation of ornithogenic nitrogen by primary producers close to the colony, increased eutrophication can not be inferred from this. No biomass measurements or community structure assessment were done, but the C:N ratios for *Acrosiphonia* sp. were notably lower at stations B2 and B3 than C2 and C3. High nitrogen content is commonly regarded as high nutritional value, suggesting better growth condition and higher nutrient availability close to the colony. The algal C:N ratios at the bird stations

are also similar to values reported from an experiment where *Acrosiphonia* from Kongsfjorden, Svalbard, was exposed to NO_3^- rich water (Hodal *et al.* 2012).

Many macroalgal species, *Acrosiphonia* included, have adapted to the seasonality of nutrient exposure at Svalbard by endogenic storage of NO_3^- when it is abundant in winter and spring. As the waters become NO_3^- depleted over summer, this reserve is used to maintain photosynthetic activity and a constant tissue C:N ratio (Hodal *et al.* 2012). Thus, the added NO_3^- flux from the seabird colony might have a larger influence on microalgae which have higher nutrient turnover. Despite this, the high $\delta^{15}N$ values from *Acrosiphina* close to Alkhornet and the higher C:N ratios found at the control sites implies a beneficial effect of the seabird colony on this algal species.

To my knowledge, previous work at Svalbard has not been conclusive on the effect of seabird nutrient subsidy on coastal ecosystems. Zmudczyńska-Skarbek *et al.* (2015) found no ornithogenic signal in the coastal benthic food web close to another mixed-colony in Isfjorden, However, the brown algae *Saccharina latissima* sampled in this study are particularly known to store nutrients endogenous over the winter, and show little effect of nutrient enrichment (Gordillo *et al.* 2006). There is also growing evidence around the world that colonies of seabirds can increase growth in coastal areas (*e.g.* Gagnon *et al.* 2015; Lorrain *et al.* 2017; Williams *et al.* 2018). On Svalbard this must be seen in the context of other processes influencing the nutrient availability. At a yearly scale, spring blooms are important in shaping the ecosystem and are likely to overshadow extra growth gained from an ornithogenic nutrient subsidy. The marine ecosystem at Alkhornet is also very dynamic and dilution of allochthonous nutrient inputs can be expected from water currents and wave action. Despite this, seeing evidence of seabird nutrient flux having an impact on the coastal food web in the few samples presented here highlight the potential of seabirds being a locally and seasonally important nutrient subsidy source.

Finally, the content of methylmercury in a selection of amphipods was analysed. Contrary to my hypothesis, the amphipods close to the colony were found to have lower concentrations of MeHg. These values are within the variation from a parallel investigation of *Gammarus setosus* in other parts of Isfjorden (Poste, unpublished data, Skogsberg 2019). The two *G. setosus* samples from the bird influenced sites are on the low end of the range observed for the broader sample set in August (2-7 ng MeHg / g d.w.), while the two *G. setosus* samples from the control sites is at the upper end of the range.

32

Ingestion is the major MeHg uptake pathway in amphipods (Taylor *et al.* 2014) and food quality can have important implications for MeHg accumulation in the species. Foraging on lower quality food can lead to higher concentrations of MeHg in the organisms, due to reduced growth rate (Lawson & Mason 1998). Amphipods close to Alkhornet feeding on phytodetritus of higher nutritional value could potentially explain the observed difference in MeHg concentrations. However, large variation in δ^{13}C was observed, pointing to variability in arctic amphipod feeding ecology. It can therefore not be excluded that the differences in mercury concentrations seen here are caused by differences in food source.

4.4 Future predictions

Both variables shaping the stream characteristics, seabird influence and runoff, are subjected to change, associated with several downstream effects on ecosystems. Svalbard is one of the places in the world experiencing climate change most strongly, a trend expected to continue in the future (Adakudlu *et al.* 2019). In addition to the predicted temperature increase of 7-10 degrees before year 2100, annual precipitation is expected to increase with 45-65% in the same period (Adakudlu *et al.* 2019). This will lead to increased runoff and more terrestrial erosion.

In parallel, many seabird populations globally have been in decline during the last decades (Croxall *et al.* 2012). While high-Arctic species like the Brünnich's guillemot show negative population development (Anker-Nilssen *et al.* 2015), more southernly species like the Northern gannet (*Morus bassanus*) range shift northwards (Barrett *et al.* 2017). Both kittiwakes and little auk have increased the foraging on Atlantic food sources on the expense of Arctic species (Vihtakari *et al.* 2018). Together, this will change the characteristics of the flux of ornithogenic nutrients and contaminants on Svalbard. The nutrient input will inevitably decline if the populations shrink. At the same time, it is possible to hypothesize that increased runoff will mobilise more of the terrestrial nutrient pool, potentially compensating in the short-term for a decreasing input. Similarly, increased runoff would lead to an increase in terrestrial mercury discharge.

5 Conclusion

The guano deposited by kittiwakes and guillemots breeding at Alkhornet have an important fertilizing effect on the nearby terrestrial environment, visible as locally high NDVI values. In the present study, we attempted to generate a preliminary nitrogen budget for the colony. From an ornithogenic deposition of nearly 30 tonnes N in the breeding season of 2018, 90-95% was estimated to be retained in the peatland. The seabird colony had a strong influence on stream water chemistry, with concentrations of TP, $NO_3^- + NO_2^-$, NH_4^+, PO_4^{3-} and TOC that were 5 to 100 fold higher here than in reference streams. A pronounced seasonality was observed in the stream parameters from snowmelt to thawing and mobilising of the soil and soil-associated compounds. Furthermore, the presence of the seabird colony also altered the mercury dynamics. TotHg was associated with organic matter in seabird influenced streams and was associated with turbidity in control streams, indicating different Hg transport pathways dominate in these different catchments. The data did not suggest any large difference in areal yield of mercury between catchments, as seabird fertilised vegetation might act a sink for mercury, counteracting the added mercury deposition from seabird transport.

A novel investigation of the response in the coastal ecosystem of these seabird derived fluxes was conducted. An ornithogenic signal (higher $\delta^{15}N$) was found in all biota collected from the seabird influenced sites. The green macroalga collected here, *Acrosiphonia* sp., had lower C:N ratios close to the colony than specimens collected from control sites. This can be explained by higher availability of nitrogen, sustaining growth during summer when nitrogen becomes limiting elsewhere. A sustained high production could explain the low MeHg concentrations observed in amphipods close to the colony, where trophic efficiency and growth dilution are important determinants for accumulation of this toxicant in the food web. The present study highlights the influence seabird colonies have on many adjacent ecosystems on Svalbard, an interaction of which we may anticipate impacts of climate change in the coming years.

6 **Further work**

Due to the novelty of research on marine response to ornithogenic fluxes on Svalbard, a preliminary approach was adapted for this study. To elucidate these processes further, there is a need for larger sample sizes at different study colonies. Complementary to the suggestions of Zmudczynska-Skarbek & Balazy (2017), areas with short distance between colony and coast as well as areas with limited water mixing should be of special interest as this is where the response should be most pronounced. A more experimental design, where periphyton communities is grown on artificial substrate during the period of meltwater could yield a more quantitate perspective on the coastal response. An attempt was done for this thesis, but unsuccessful as all rigs were washed away (Appendix G)

7 References

Adakudlu, M., Andresen, J., Bakke, J., Beldring, S., & Renestad, W. (2019, January). Climate in Svalbard 2100 – a knowledge base for climate adaptation., Norwegian Environment Agency.

Anderson, S. P. (2005). Glaciers show direct linkage between erosion rate and chemical weathering fluxes. *Geomorphology*, **67**(1), 147–157.

Anker-Nilssen, T., Barrett, R., Christensen-Dalsgaard, S., Hanssen, S. A., Reiertsen, T. K., Bustnes, J. O., Erikstad, K.-E., Follestad, A., Langset, M., Lorentsen, S.-H., Lorentzen, E., Strøm, H., & Systad, G. H. (2018). Key-site monitoring in Norway 2017, including Svalbard and Jan Mayen, 14.

Anker-Nilssen, T., Barrett, R. T., Christensen-Dalsgaard, S., Descamps, S., & Strøm, H. (2015). SEAPOP De ti første årene. Nøkkeldokument 2005-2014. *Norsk institutt for naturforskning, Norsk Polarinstitutt & Tromsø Museum*, 58.

Banerjee, S., & Siciliano, S. D. (2012). Factors driving potential ammonia oxidation in canadian Arctic ecosystems: does spatial scale matter? *Applied and Environmental Microbiology*, **78**(2), 346–353.

Barrett, R. T., Anker-Nilssen, T., Gabrielsen, G. W., & Chapdelaine, G. (2002). Food consumption by seabirds in Norwegian waters. *ICES Journal of Marine Science*, **59**(1), 43–57.

Barrett, R. T., Strøm, H., & Melnikov, M. (2017). On the polar edge: the status of the northern gannet (*Morus bassanus*) in the Barents Sea in 2015-16. *Polar Research*, **36**(1), 1390384.

Bechmann, M. (2014). Long-term monitoring of nitrogen in surface and subsurface runoff from small agricultural dominated catchments in Norway. *Agriculture, Ecosystems & Environment*, **198**, 13–24.

Berchenko, I. V., Ezhov, A. V., & Oleinik, A. A. (2017). On the issue of influence of coastal seabird colonies on adjacent pelagic communities of the Kola Peninsula. *Russian Journal of Marine Biology*, **43**(4), 312–315.

Blais, J. M., Kimpe, L. E., McMahon, D., & Smol, J. P. (2005). Arctic seabirds transport marine-derived contaminants. *Science*, **309**(5733), 445–445.

Bouchard Marmen, M., Kenchington, E., Ardyna, M., & Archambault, P. (2017). Influence of seabird colonies and other environmental variables on benthic community structure, Lancaster Sound Region, Canadian Arctic. *Journal of Marine Systems*, **167**(Supplement C), 105–117.

Braaten, H. F. V., Harman, C., Øverjordet, I. B., & Larssen, T. (2014a). Effects of sample preparation on methylmercury concentrations in Arctic organisms. *International Journal of Environmental Analytical Chemistry*, **94**(9), 863–873.

Braaten, H. F. V., Wit, H. A. de, Harman, C., Hageström, U., & Larssen, T. (2014b). Effects of sample preservation and storage on mercury speciation in natural stream water. *International Journal of Environmental Analytical Chemistry*, **94**(4), 381–384.

Breuning-Madsen, H., Ehlers-Koch, C., Gregersen, J., & Løjtnant, C. L. (2010). Influence of perennial colonies of piscivorous birds on soil nutrient contents in a temperate humid climate. *Geografisk Tidsskrift-Danish Journal of Geography*, **110**(1), 25–35.

Brodie, C. R., Leng, M. J., Casford, J. S. L., Kendrick, C. P., Lloyd, J. M., Yongqiang, Z., & Bird, M. I. (2011). Evidence for bias in C and N concentrations and δ13C composition of terrestrial and aquatic organic materials due to pre-analysis acid preparation methods. *Chemical Geology*, **282**(3), 67–83.

Burr, Z. M., Varpe, Ø., Anker-Nilssen, T., Erikstad, K. E., Descamps, S., Barrett, R. T., Bech, C., Christensen-Dalsgaard, S., Lorentsen, S.-H., Moe, B., Reiertsen, T. K., & Strøm, H. (2016). Later at higher latitudes: large-scale variability in seabird breeding timing and synchronicity. *Ecosphere*, **7**(5), e01283.

Camphuysen, C. J., & den Ouden, J. E. (1995). De broedvogels van Alkhornet, West-Spitsbergen. *Sula*, **9**(3), 119–123.

Carlson, T. N., & Ripley, D. A. (1997). On the relation between NDVI, fractional vegetation cover, and leaf area index. *Remote Sensing of Environment*, **62**(3), 241–252.

Choy, E. S., Kimpe, L. E., Mallory, M. L., Smol, J. P., & Blais, J. M. (2010). Contamination of an arctic terrestrial food web with marine-derived persistent organic pollutants transported by breeding seabirds. *Environmental Pollution*, **158**(11), 3431–3438.

Croxall, J. P., Butchart, S. H. M., Lascelles, B., Stattersfield, A. J., Sullivan, B., Symes, A., & Taylor, P. (2012). Seabird conservation status, threats and priority actions: a global assessment. *Bird Conservation International*, **22**(1), 1–34.

Dallmann, W. K. (2002). Bedrock map of Svalbard and Jan Mayen: Berggrunnskart over Svalbard og Jan Mayen, Oslo: Norsk Polarinstitutt.

Descamps, S., Strøm, H., & Steen, H. (2013). Decline of an arctic top predator: synchrony in colony size fluctuations, risk of extinction and the subpolar gyre. *Oecologia*, **173**(4), 1271–1282.

Dodds, W. K., López, A. J., Bowden, W. B., Gregory, S., Grimm, N. B., Hamilton, S. K., Hershey, A. E., Martí, E., McDowell, W. H., Meyer, J. L., Morrall, D., Mulholland, P. J., Peterson, B. J., Tank, J. L., Valett, H. M., Webster, J. R., & Wollheim, W. (2002). N uptake as a function of concentration in streams. *Journal of the North American Benthological Society*, **21**(2), 206–220.

Duda, M. P., Hargan, K. E., Michelutti, N., Kimpe, L. E., Clyde, N., Gilchrist, H. G., Mallory, M. L., Blais, J. M., & Smol, J. P. (2018). Breeding eider ducks strongly influence subarctic coastal pond chemistry. *Aquatic Sciences*, **80**(4), 40.

Dunn, R. E., White, C. R., & Green Jonathan A. (2018). A model to estimate seabird field metabolic rates. *Biology Letters*, **14**(6), 20180190.

Durnford, D., Dastoor, A., Figueras-Nieto, D., & Ryjkov, A. (2010). Long range transport of mercury to the Arctic and across Canada. *Atmospheric Chemistry and Physics*, **10**(13), 6063–6086.

Eide, N. E., Eid, P. M., Prestrud, P., & Swenson, J. E. (2005). Dietary responses of Arctic foxes *Alopex lagopus* to changing prey availability across an Arctic landscape. *Wildlife Biology*, **11**(2), 109–121.

Førland, E. J., & Hanssen-Bauer, I. (2000). Increased precipitation in the Norwegian Arctic: true or false? *Climatic Change*, **46**(4), 485–509.

Frank, D. A., Evans, R. D., & Tracy, B. F. (2004). The role of ammonia volatilization in controlling the natural ^{15}N abundance of a grazed grassland. *Biogeochemistry*, **68**(2), 169–178.

Gagnon, K., Yli-Rosti, J., & Jormalainen, V. (2015). Cormorant-induced shifts in littoral communities. *Marine Ecology Progress Series*, **541**, 15–30.

Galloway, J. N., Dentener, F. J., Capone, D. G., Boyer, E. W., Howarth, R. W., Seitzinger, S. P., Asner, G. P., Cleveland, C. C., Green, P. A., Holland, E. A., Karl, D. M., Michaels, A. F., Porter, J. H., Townsend, A. R., & Vöosmarty, C. J. (2004). Nitrogen Cycles: Past, present, and future. *Biogeochemistry*, **70**(2), 153–226.

Glibert, P. M., Wilkerson, F. P., Dugdale, R. C., Raven, J. A., Dupont, C. L., Leavitt, P. R., Parker, A. E., Burkholder, J. M., & Kana, T. M. (2016). Pluses and minuses of ammonium and nitrate uptake and assimilation by phytoplankton and implications for productivity and community composition, with emphasis on nitrogen-enriched conditions. *Limnology and Oceanography*, **61**(1), 165–197.

González-Bergonzoni, I., Johansen, K. L., Mosbech, A., Landkildehus, F., Jeppesen, E., & Davidson, T. A. (2017). Small birds, big effects: the little auk (*Alle alle*) transforms high Arctic ecosystems. *Proc. R. Soc. B*, **284**(1849), 20162572.

Gordillo, F. J. L., Aguilera, J., & Jiménez, C. (2006). The response of nutrient assimilation and biochemical composition of Arctic seaweeds to a nutrient input in summer. *Journal of Experimental Botany*, **57**(11), 2661–2671.

Graham, N. A. J., Wilson, S. K., Carr, P., Hoey, A. S., Jennings, S., & MacNeil, M. A. (2018). Seabirds enhance coral reef productivity and functioning in the absence of invasive rats. *Nature*, **559**(7713), 250.

GRASS Development Team. (2017). *Geographic Resources Analysis Support System (GRASS GIS) Software, Version 7.2*, Open Source Geospatial Foundation. Retrieved from http://grass.osgeo.org

Greenacre, M., & Primicerio, R. (2014). *Multivariate analysis of ecological data*, Bilbao, Spain: Fundación BBVA.

Harding, J. S., Hawke, D. J., Holdaway, R. N., & Winterbourn, M. J. (2004). Incorporation of marine-derived nutrients from petrel breeding colonies into stream food webs. *Freshwater Biology*, **49**(5), 576–586.

Hintelmann, H., & Nguyen, H. T. (2005). Extraction of methylmercury from tissue and plant samples by acid leaching. *Analytical and Bioanalytical Chemistry*, **381**(2), 360–365.

Hodal, H., Falk-Petersen, S., Hop, H., Kristiansen, S., & Reigstad, M. (2012). Spring bloom dynamics in Kongsfjorden, Svalbard: nutrients, phytoplankton, protozoans and primary production. *Polar Biology*, **35**(2), 191–203.

Jakubas, D., Zmudczyńska, K., Wojczulanis-Jakubas, K., & Stempniewicz, L. (2008). Faeces deposition and numbers of vertebrate herbivores in the vicinity of planktivorous and piscivorous seabird colonies in Hornsund, Spitsbergen. *Polish Polar Research*, **29**(1), 14.

Johansen, B., & Tømmervik, H. (2014). The relationship between phytomass, NDVI and vegetation communities on Svalbard. *International Journal of Applied Earth Observation and Geoinformation*, **27**, 20–30.

Johansen, B., Tømmervik, H., & Karlsen, S. R. (2009). *Vegetasjonskart over Svalbard basert på satellittdata. Dokumentasjon av metoder og vegetasjonsbeskrivelser* (No. 456), Norsk institutt for naturforskning. Retrieved from https://brage.bibsys.no/xmlui/handle/11250/2388746

Kaste, Ø., Skarbøvik, E., Greipsland, I., Gundersen, C. B., Austnes, K., Skancke, L. B., Guerrero, J.-L., & Sample, J. E. (2018). *The Norwegian river monitoring programme – water quality status and trends 2017* (No. 7313–2018), Norsk institutt for vannforskning. Retrieved from https://brage.bibsys.no/xmlui/handle/11250/2588692

Killingtveit, Å., Pettersson, L.-E., & Sand, K. (2003). Water balance investigations in Svalbard. *Polar Research*, **22**(2), 161–174.

Kristiansen, S. M. (2017). *The exposure and accumulation of seabird-derived contaminants and genotoxicity in Collembola from Svalbard* (Master's thesis), University of Oslo, Oslo. Retrieved from https://www.duo.uio.no/handle/10852/60816

Låg, J. (1990). Peat accumulation in steep hills at Alkhornet, Spitsbergen. *Acta Agriculturae Scandinavica*, **40**(3), 217–219.

Lawson, N. M., & Mason, R. P. (1998). Accumulation of mercury in estuarine food chains. *Biogeochemistry*, **40**, 235–247.

Leblans, N. I. W., Sigurdsson, B. D., Roefs, P., Thuys, R., Magnússon, B., & Janssens, I. A. (2014). Effects of seabird nitrogen input on biomass and carbon accumulation after 50 years of primary succession on a young volcanic island, Surtsey. *Biogeosciences*, **11**(22), 6237–6250.

Legeżyńska, J., Kędra, M., & Walkusz, W. (2012). When season does not matter: summer and winter trophic ecology of Arctic amphipods. *Hydrobiologia*, **684**(1), 189–214.

Lehnherr, I. (2014). Methylmercury biogeochemistry: a review with special reference to Arctic aquatic ecosystems. *Environmental Reviews*, **22**(3), 229–243.

Lorrain, A., Houlbrèque, F., Benzoni, F., Barjon, L., Tremblay-Boyer, L., Menkes, C., Gillikin, D. P., Payri, C., Jourdan, H., Boussarie, G., Verheyden, A., & Vidal, E. (2017). Seabirds supply nitrogen to reef-building corals on remote Pacific islets. *Scientific Reports*, **7**. doi:10.1038/s41598-017-03781-y

Nilsen, F., Cottier, F., Skogseth, R., & Mattsson, S. (2008). Fjord–shelf exchanges controlled by ice and brine production: The interannual variation of Atlantic Water in Isfjorden, Svalbard. *Continental Shelf Research*, **28**(14), 1838–1853.

Olson, M. L., & DeWild, J. F. (1997). *Determination of total mercury in water by oxidation, purge and trap, and cold vapor atomic fluorescence spectrometry*.

Otero, X. L., Peña-Lastra, S., Pérez-Alberti, A., Ferreira, T. O., & Huerta-Diaz, M. A. (2018). Seabird colonies as important global drivers in the nitrogen and phosphorus cycles. *Nature Communications*, **9**(1), 246.

Paleczny, M., Hammill, E., Karpouzi, V., & Pauly, D. (2015). Population trend of the world's monitored seabirds, 1950-2010. *PLOS ONE*, **10**(6), e0129342.

Parsons, M., Mitchell, I., Butler, A., Ratcliffe, N., Frederiksen, M., Foster, S., & Reid, J. B. (2008). Seabirds as indicators of the marine environment. *ICES Journal of Marine Science*, **65**(8), 1520–1526.

Peterson, B. J., & Fry, B. (1987). Stable Isotopes in Ecosystem Studies. *Annual Review of Ecology and Systematics*, **18**(1), 293–320.

Pickhardt, P. C., Folt, C. L., Chen, C. Y., Klaue, B., & Blum, J. D. (2002). Algal blooms reduce the uptake of toxic methylmercury in freshwater food webs. *Proceedings of the National Academy of Sciences*, **99**(7), 4419–4423.

Pitcairn, C. E. R., Skiba, U. M., Sutton, M. A., Fowler, D., Munro, R., & Kennedy, V. (2002). Defining the spatial impacts of poultry farm ammonia emissions on species composition of adjacent woodland groundflora using Ellenberg Nitrogen Index, nitrous oxide and nitric oxide emissions and foliar nitrogen as marker variables. *Environmental Pollution*, **119**(1), 9–21.

Poncea, V. M., & Shetty, A. V. (1995). A conceptual model of catchment water balance: 1. Formulation and calibration. *Journal of Hydrology*, **173**(1), 27–40.

QGIS Development Team. (2019). *QGIS Geographic Information System. Project, Version 3.4.3*, Open Source Geospatial Foundation. Retrieved from http://qgis.osgeo.org

Reynolds, C. S., & Davies, P. S. (2001). Sources and bioavailability of phosphorus fractions in freshwaters: a British perspective. *Biological Reviews*, **76**(1), 27–64.

Richter, D., Matuła, J., Urbaniak, J., Waleron, M., & Czerwik-Marcinkowska, J. (2017). Molecular, morphological and ultrastructural characteristics of *Prasiola crispa* (Lightfoot) Kützing (Chlorophyta) from Spitsbergen (Arctic). *Polar Biology*, **40**(2), 379–397.

Riddick, S. N., Dragosits, U., Blackall, T. D., Daunt, F., Wanless, S., & Sutton, M. A. (2012). The global distribution of ammonia emissions from seabird colonies. *Atmospheric Environment*, **55**, 319–327.

Rousk, K., Sorensen, P. L., & Michelsen, A. (2017). Nitrogen fixation in the High Arctic: a source of 'new' nitrogen? *Biogeochemistry*, **136**(2), 213–222.

Shatova, O. A., Wing, S. R., Hoffmann, L. J., Wing, L. C., & Gault-Ringold, M. (2017). Phytoplankton community structure is influenced by seabird guano enrichment in the Southern Ocean. *Estuarine, Coastal and Shelf Science*, **191**(Supplement C), 125–135.

Shotyk, W. (2017). Biogeochemistry: Arctic plants take up mercury vapour. *Nature*, **547**(7662), 167–168.

Skogsberg, E. (2019). *Effects of seasonal riverine run-off on coastal contaminant levels in Arctic littoral amphipods* (Master's thesis), University of Oslo, Oslo.

Smoła, Z. T., Tatarek, A., Wiktor, J. M., Wiktor, J. M. W., Kubiszyn, A., & Węsławski, J. M. (2017). Primary producers and production in Hornsund and Kongsfjorden – comparison of two fjord systems. *Polish Polar Research*, **38**(3), 351–373.

Sokołowski, A., Szczepańska, A., Richard, P., Kędra, M., Wołowicz, M., & Węsławski, J. M. (2014). Trophic structure of the macrobenthic community of Hornsund, Spitsbergen, based on the determination of stable carbon and nitrogen isotopic signatures. *Polar Biology*, **37**(9), 1247–1260.

Søreide, J. E., & Nygård, H. (2012). Challenges using stable isotopes for estimating trophic levels in marine amphipods. *Polar Biology*, **35**(3), 447–453.

Taylor, V. F., Bugge, D., Jackson, B. P., & Chen, C. Y. (2014). Pathways of CH3Hg and Hg Ingestion in Benthic Organisms: An Enriched Isotope Approach. *Environmental Science & Technology*, **48**(9), 5058–5065.

Tranter, M., Sharp, M. J., Lamb, H. R., Brown, G. H., Hubbard, B. P., & Willis, I. C. (2002). Geochemical weathering at the bed of Haut Glacier d'Arolla, Switzerland?a new model. *Hydrological Processes*, **16**(5), 959–993.

Turetsky, M. R. (2003). The Role of Bryophytes in Carbon and Nitrogen Cycling. *The Bryologist*, **106**(3), 395–409.

Vihtakari, M., Welcker, J., Moe, B., Chastel, O., Tartu, S., Hop, H., Bech, C., Descamps, S., & Gabrielsen, G. W. (2018). Black-legged kittiwakes as messengers of Atlantification in the Arctic. *Scientific Reports*, **8**(1), 1178.

Vitousek, P. M., Menge, D. N. L., Reed, S. C., & Cleveland, C. C. (2013). Biological nitrogen fixation: rates, patterns and ecological controls in terrestrial ecosystems. *Philosophical Transactions of the Royal Society B: Biological Sciences*, **368**(1621), 20130119.

Wainright, S. C., Haney, J. C., Kerr, C., Golovkin, A. N., & Flint, M. V. (1998). Utilization of nitrogen derived from seabird guano by terrestrial and marine plants at St. Paul, Pribilof Islands, Bering Sea, Alaska. *Marine Biology*, **131**(1), 63–71.

Williams, J. J., Papastamatiou, Y. P., Caselle, J. E., Bradley, D., & Jacoby, D. M. P. (2018). Mobile marine predators: an understudied source of nutrients to coral reefs in an unfished atoll. *Proc. R. Soc. B*, **285**(1875), 20172456.

Wilson, L. J., Bacon, P. J., Bull, J., Dragosits, U., Blackall, T. D., Dunn, T. E., Hamer, K. C., Sutton, M. A., & Wanless, S. (2004). Modelling the spatial distribution of ammonia emissions from seabirds in the UK. *Environmental Pollution*, **131**(2), 173–185.

Witherby, H. F. (1963). *The Handbook of British Birds.*, London: H. F. & G. Witherby LTD.

Yano, Y., Shaver, G. R., Giblin, A. E., Rastetter, E. B., & Nadelhoffer, K. J. (2010). Nitrogen dynamics in a small arctic watershed: retention and downhill movement of 15 N. *Ecological Monographs*, **80**(2), 331–351.

Yeh, K. C., & Kwan, K. C. (1978). A comparison of numerical integrating algorithms by trapezoidal, Lagrange, and spline approximation. *Journal of Pharmacokinetics and Biopharmaceutics*, **6**(1), 79–98.

Zmudczynska-Skarbek, K., & Balazy, P. (2017). Following the flow of ornithogenic nutrients through the Arctic marine coastal food webs. *Journal of Marine Systems*, **168**, 31–37.

Zmudczyńska-Skarbek, K., Balazy, P., & Kuklinski, P. (2015). An assessment of seabird influence on Arctic coastal benthic communities. *Journal of Marine Systems*, **144**(Supplement C), 48–56.

Zwolicki, A., Zmudczyńska-Skarbek, K., Matuła, J., Wojtuń, B., & Stempniewicz, L. (2016). Differential responses of Arctic vegetation to nutrient enrichment by plankton- and fish-eating colonial seabirds in Spitsbergen. *Frontiers in Plant Science*, **7**. doi:10.3389/fpls.2016.01959

8 Appendices

Appendix A: Overview of analytic methods

Table A1: Overview of methods used in analysis of water-chemistry at NIVA (MeHg analysed at the Environmental Science and Analytic Chemistry Department of Stockholm University). From (Braaten et al. 2014a; Hintelmann & Nguyen 2005; Kaste et al. 2018)

Parameter	Analytic method	
TOC	NS 1484 modified	Spectrophotometry
TP	NS 4725	Spectrophotometry (Peroxodisulphate oxidation method modified)
PO_4^{3-}-P	NS 4724	Spectrophotometry (Automated molybdate method modified)
TN	NS 4743	Spectrophotometry
NO_3^--N + NO_2^--N	NS-EN ISO 10304-1	Ion chromatography
NH_4^+-N	NS-EN ISO 14911	Ion chromatography
SiO2	NS-EN ISO 16264 modified	Spectrophotometry
TotHg	USEPA Method 1631	Oxidation, purge and trap, and cold vapor atomic fluorescence spectrometry
MeHg	USEPA Method 1630	Distillation, aqueous ethylation, purge and trap, and cold vapor atomic fluorescence spectrometry

Appendix B: Runoff estimation
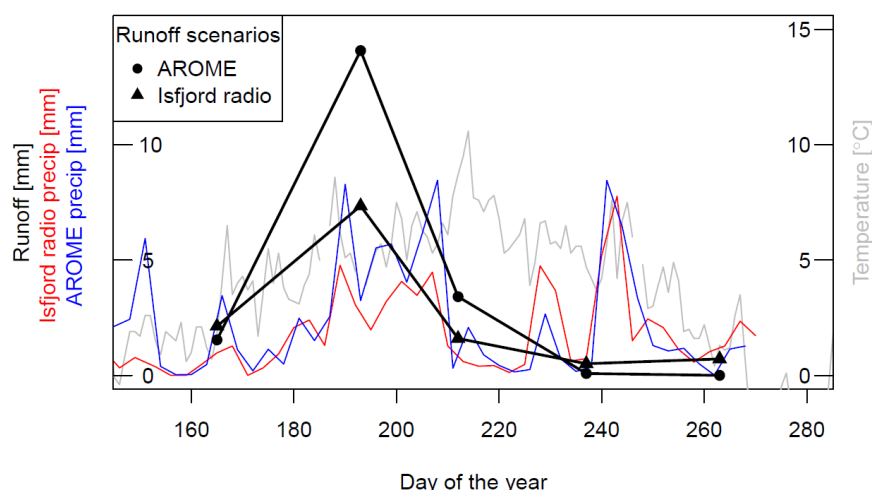
Figure A1: Temperature, precipitation and runoff scenarios in the sampling period. The grey line shows the daily temperature averages at Isfjord Radio, the red line is drawn between three-day averages of precipitation at Isfjord radio and the blue line between three day averages from AROME. The black line with triangle symbols show the runoff estimates from Isfjord radio data when snow melt is accounted for, and similarly are the black circles from AROME runoff estimates.

Appendix C: Stream stations
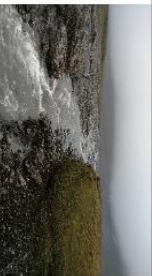
Figure A2: Overview of the water level in all stream stations. A 5L carboy is included in some pictures for scale.

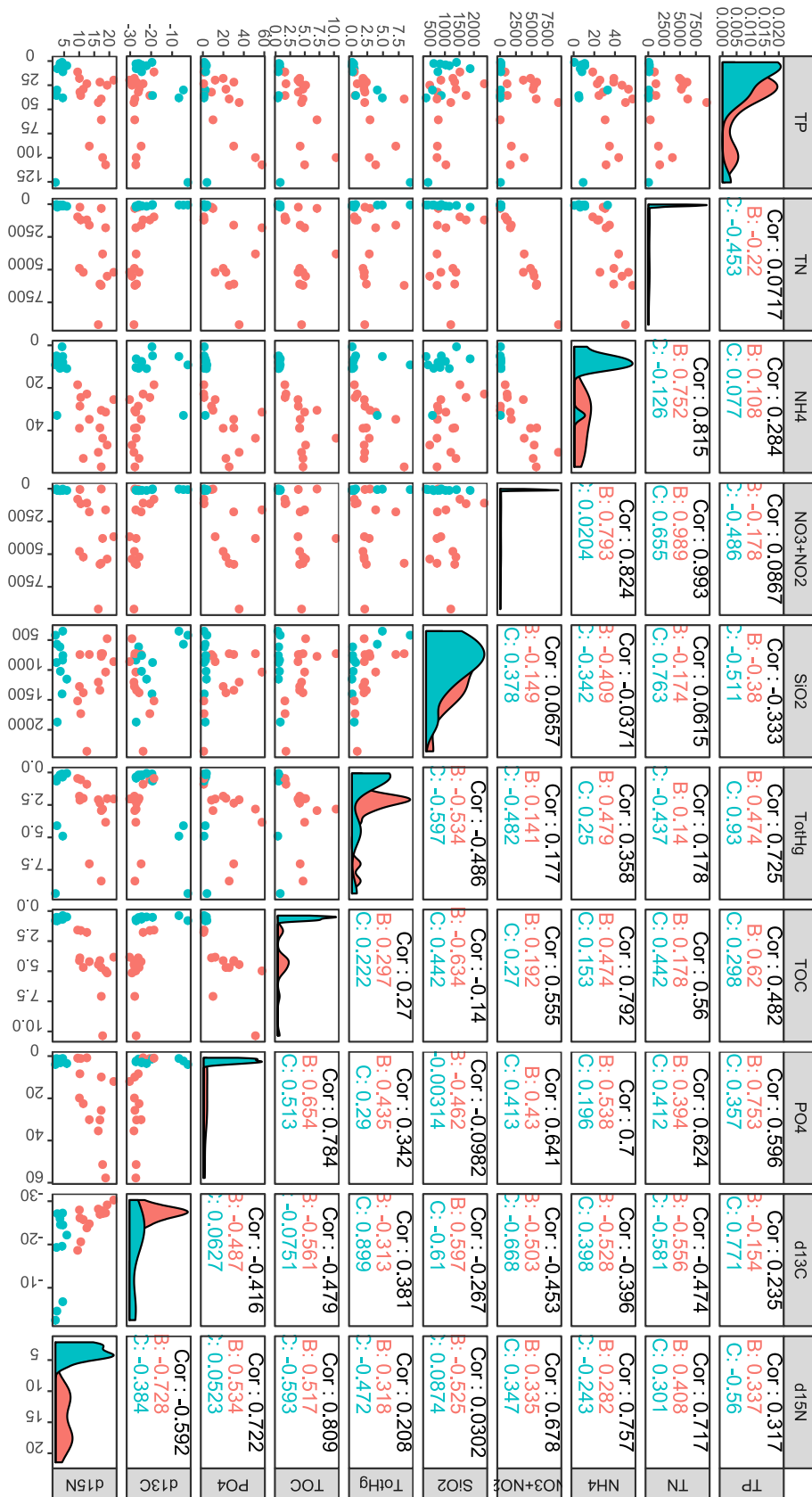# Appendix D: correlation plots

Figure A3: correlation plot of all stream water-chemistry parameters and SI. Black "Cor" indicates the correlation for both seabird and control streams, while red B is only for seabird stream, and blue C is for controls
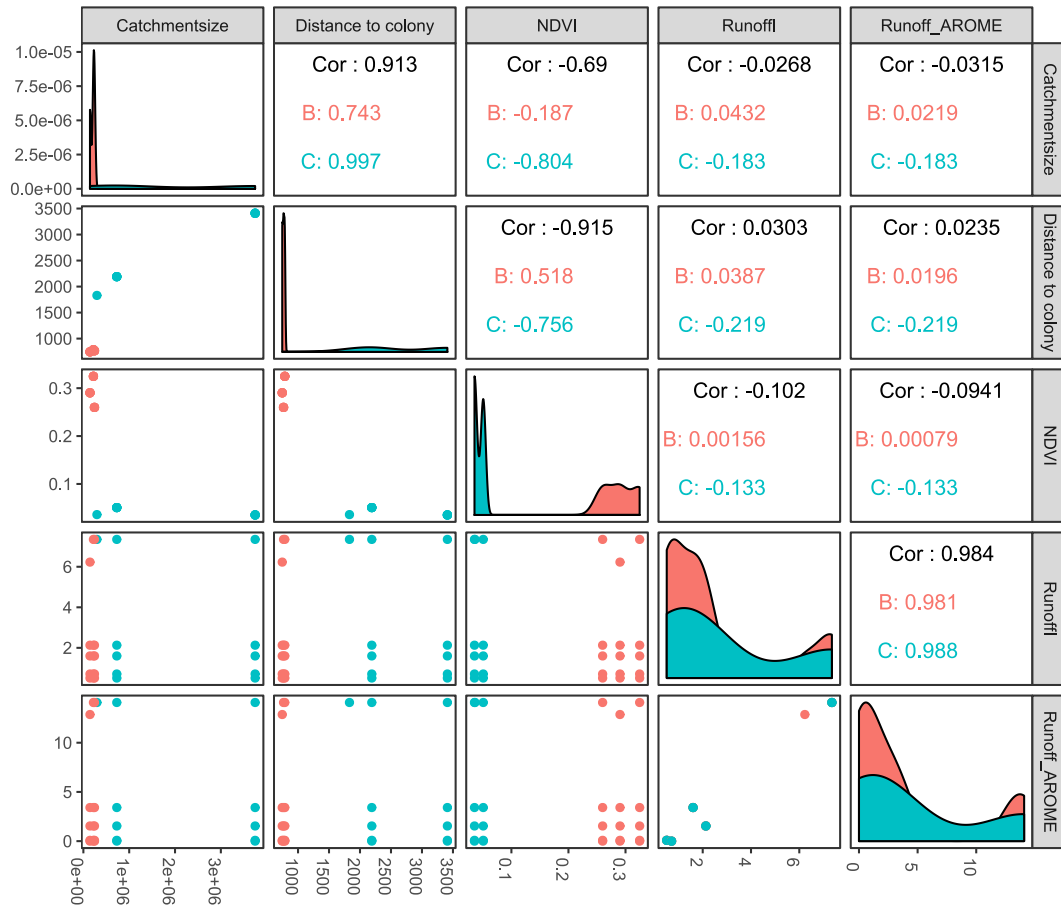
Figure A4: correlation plot of environmental predictors. Black "Cor" indicates the correlation for both seabird and control streams, while red B is only for seabird stream, and blue C is for controls

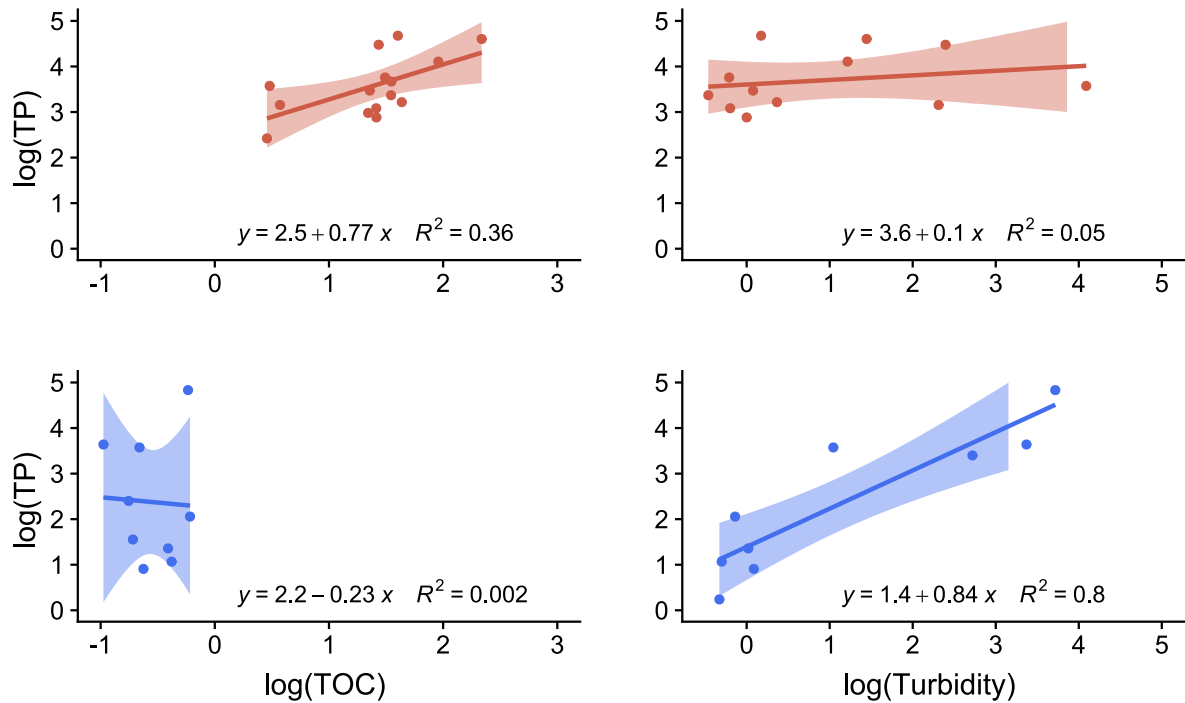# Appendix E: Drivers of TP concentration in streams

Figure 6: Regression of TP in streams predicted by TOC and turbidity for bird influenced streams (red, top) and control streams (blue, bottom). All variables are log transformed to achieve a normal distribution. See Figure 4 for untransformed values.
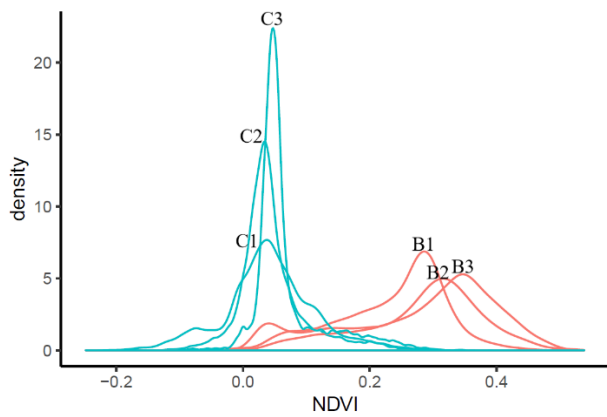
Appendix F: NDVI

Figure A6: Density plot of NDVI values from 10 000 random sampled pixels in each catchment, the red being seabird influenced, and blue being control catchments.
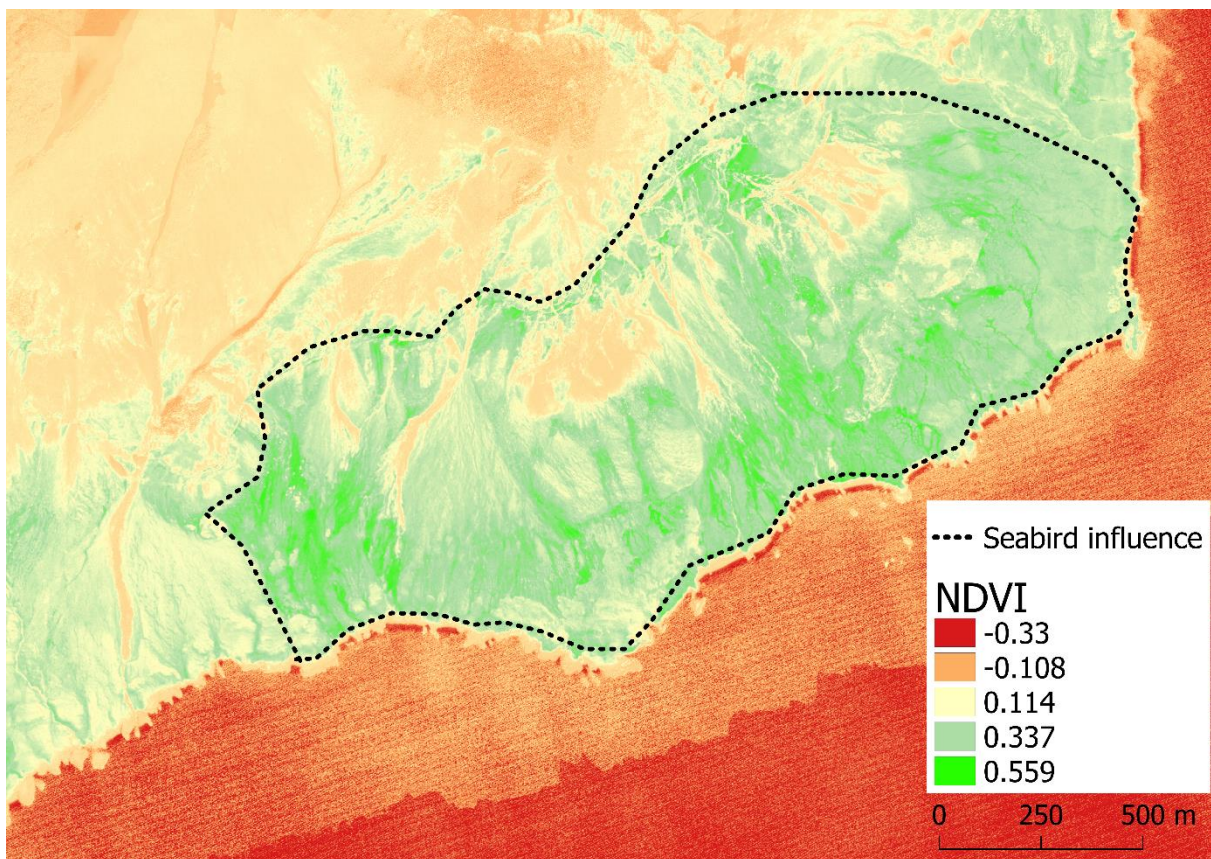

Figure A7: NDVI heatmap for the area around Alkhornet. The area displaying particularly high NDVI values are delineated with black dotted line, covering an area of 1.8 km^2 of assumingly seabird influenced vegetation.

Appendix G: Periphyton rigs

At the first sampling in June, a rig with 5 plexiglass tiles were deployed outside each of the stations by snorkelling. The plexiglass tiles were 15x15cm and roughed with sandpaper. Two tiles were bound to an anchor, made from a heavy piece of rebar, while the other three were suspended 40 cm above the bottom in a triangle (Figure A1). The depth of deployment ranged from 4 to 7 meters between stations, and 30-60 meters off the coast. These rigs were left for periphyton to attach and grow, before being collected in the fall and analysed for seabird influence. Unfortunately, the anchors were unable to secure the rigs and all 6 were gone when we searched for them in August and September.
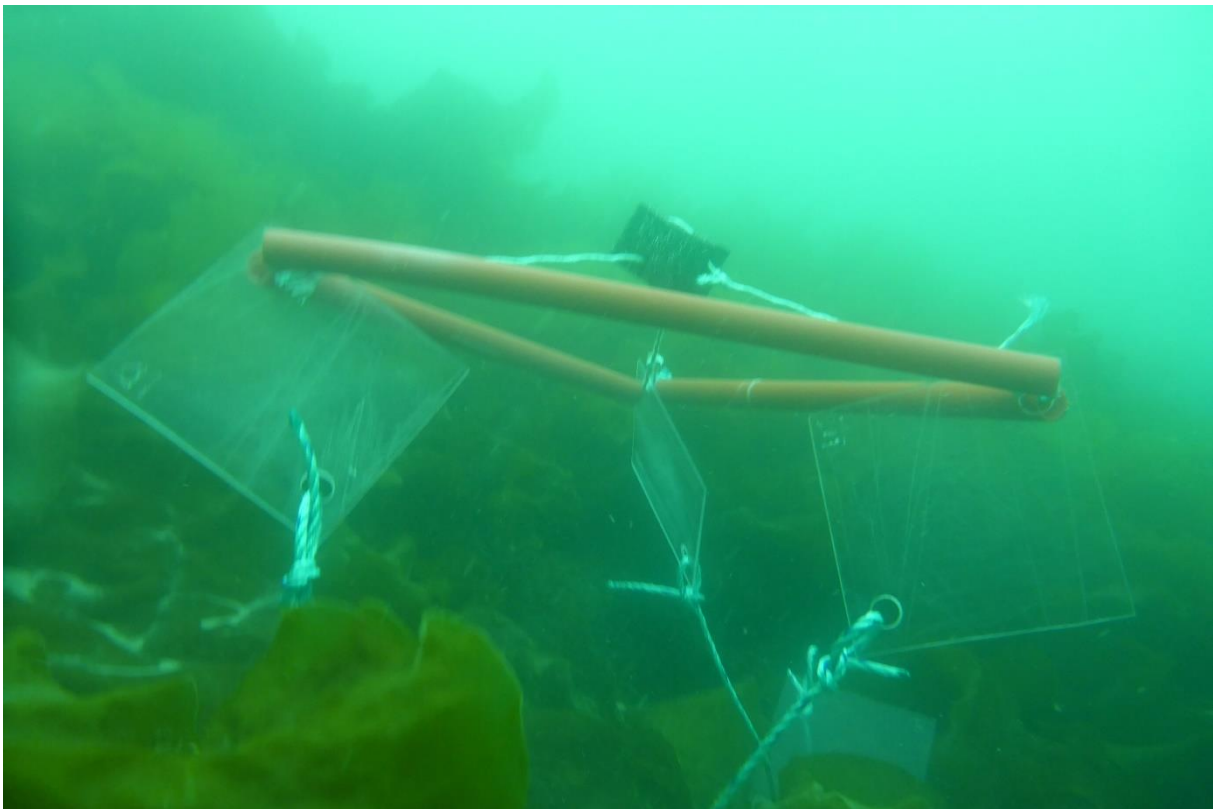

Figure A8: The periphyton rig deployed at station C1. The three suspended tiles are visible in the centre of the picture, while one of the three bottom tiles can be discerned in the bottom centre-right partly covered by the kelp forest.